Effect of particle size and natural organic matter on the transport and fate of latex nanoparticles in saturated porous media

Andrew John Pelley

Department of Chemical Engineering

McGill University, Montreal

September 28th, 2007

A thesis submitted to McGill University

in partial fulfillment of the degree of Masters of Engineering

Your file Votre référence
ISBN: 978-0-494-38492-3
Our file Notre référence
ISBN: 978-0-494-38492-3

Abstract

Colloid filtration experiments were performed using latex particles (50 nm, 110 nm and 1500 nm) in both the presence and absence of 5.0 mg/L humic acid (HAs). At low ionic strengths (1 – 10 mM KCl), an increase in attachment efficiency (α) with increasing particle size was observed, which contrasts with predictions based on DLVO theory. The presence of HAs generally resulted in a decrease in α. Characterization experiments to better understand this behaviour included particle sizing using dynamic light scattering (DLS) and zeta potential using laser Doppler velocimetry (LDV). The particles' hydrodynamic diameters were unchanged in the presence of HAs. HAs lead to an increase in absolute zeta potential for the 50 nm and 110 nm colloids and a decrease in zeta potential for the 1500 nm particles. A discussion of the apparent deviations from Derjaguin-Landau-Verwey-Overbeek (DLVO) theory and explanations for the observed behaviour are provided.

Abstract

Des expériences de filtration des colloïdes ont été effectuées en utilisant des particules de latex (50, 110 et 1500 nm) en présence ou sans 5.0 mg/L d'acides humiques (AH). A basse force ionique (1 – 10 mM KCl), une augmentation de l'efficacité d'attachement (α) avec l'augmentation de la taille des particules a été observé, ce qui contredit les prédictions basées sur la théorie DLVO. La présence d'AH résultait généralement en une baisse d'α. Pour mieux comprendre les tendances observées, des expériences de charactérization incluant la mesure du diamètre des particules utilisant DLS et le potentiel zéta utilisant LDV. Le diamètre hydrodynamique des particules demeure stable en présence des AH. Les AH augmentent le potentiel zéta absolu pour les colloïdes de 50 et 110 nm et une baisse en potentiel zéta pour les particules de 1500 nm. Une discussion des différences apparentes avec la théorie DLVO et des explications des tendances observées sont données.

Acknowledgements

Foremost, I would like to acknowledge Dr. Nathalie Tufenkji for having given me this opportunity to further my education, for securing the funding required and for her guidance and assistance throughout the course of this research project.

Second, I would like to thank the generous contributors to the Eugenie-Ulmer-Lamothe fund for their involvement in the academic formation of so many young engineers and for helping to maintain the venerable reputation of the McGill Chemical Engineering department as a place of learning and professional development. I would also like to acknowledge the Natural Sciences and Engineering Research Council of Canada for the support that they provide to young professors in the establishment of new research groups, because these initial funds help to remove the barriers to entry into academic research.

Last, but certainly not least, I would like to acknowledge two of the members of our young research group, Felipe Castro and Charles Poitras, for having been sounding boards for my thoughts and frustrations throughout my tenure at McGill and for all of their invaluable support.

Table of Contents

List of Figures

List of Tables

1.0 Background and Motivation

1.1 History and Environmental Relevance

Dutch scientist Anton van Leeuwenhoek first observed bacteria in 1674 using a microscope of his own design [1]. Though he likely didn't appreciate their significance at the time, those early observations helped pave the way for bioengineering and by 1862 Louis Pasteur and Claude Bernard were recognizing the potential for harnessing these microscopic organisms [2]. With the invention of new analytical and imaging techniques, humans began to exert their control over things on a progressively smaller scale. In 1953, James D. Watson and Francis Crick made use of crucial x-ray diffraction images to propose a model for the structure of DNA and allowed for the characterization of the building blocks of life [3]. Further innovations are leading towards a future wherein humans will likely be able to control the manufacture of materials and perhaps life itself on an atom-by-atom or molecule-by-molecule basis. Currently, materials are being manufactured that have characteristic dimensions which are smaller than 100 nm and this newfound ability to tailor materials on the nanoscale has lead to the development of a flourishing nanomaterials sector creating products for a wide range of consumer and industrial applications.

To prevent health and environmental consequences that may become associated with these products throughout their life-cycle, an urgent need exists to consider the possible implications of nanomaterial fabrication. If not, the production, use and eventual disposal of nanomaterials will invariably lead to their presence in air, water and soils. Conscientious use of nanomaterials will require a better understanding of their mobility, bioavailability and toxicity prior to their widespread development to assess the associated risks.

Early research efforts have largely focused on hazards associated with exposure to nanomaterials, particularly to those involved in the fabrication of these materials [4]. This exposure can occur through the skin, the lungs and the gastrointestinal tract. While meticulous workplace handling of materials and proper disposal of wastes may help to limit human exposure, there is still insufficient information regarding the partitioning of

these particles into various phases (e.g. air and water) and the mobility and persistence of nanomaterials in the environment. Furthermore, while regulations controlling the disposal of wastes are often drafted in terms of mass concentrations, a growing body of evidence suggests that the physicochemical properties of a material that are most strongly linked to its toxicity are its surface area, size, acidity and metal content [4]. Due to their relatively small size, a given mass of nanomaterials will have a much larger specific surface area than micron-sized particulates and hence have much more potential for toxicity. As a result, if emission standards for nanomaterials are to be appropriate, they would best be stated in terms of surface area or number concentration.

Initial investigations into the mobility of nanomaterials in systems that resemble groundwater aquifers have found that mobility is a function of both surface chemistry [5] and particle size [6-8] and that varying the functionalization of a given nanoparticle can lead to significant differences in that particle's mobility [9, 10]. For example, nanoparticulate fullerene aggregates (nC_{60}) have very limited mobility in porous media due to their low solubility in water while fullerol has been found to be highly mobile [11]. Findings such as these underscore the need to avoid using generalizations in the implementation of a regulatory environmental framework for nanomaterials.

Intuitively, many assume that given their small size, nanoparticles will be highly mobile in aquatic environments. Classical colloid filtration theory states that, all other properties being equal, the mobility of very small particles should be limited because their high diffusivities should lead to a higher incidence of collisions with the surface of granular materials such as sand grains. However, some of the short-range forces (e.g., structural or hydration forces, diffuse-layer interactions, steric interactions) that are often neglected in standard colloidal interactions may become relevant over the length scales involved in nanoparticle deposition [4]. This and other factors may lead to large discrepancies between the actual and predicted mobility of nanoparticles in the subsurface and are the reasons why further study of nanoparticle transport and fate in subsurface environments is required.

1.2 Colloid Filtration Theory

Prior to examining the transport and fate of anthropogenic nanomaterials in saturated porous media, it is important to first gain an understanding of the mechanisms that are involved in the contact and potential attachment of nanoparticles to an individual collector (i.e. sand grain). When a fluid streamline passes close to the surface of an individual collector within a granular porous matrix, there is a possibility that particles entrained within that streamline will come sufficiently close to the collector to contact its surface. It is generally accepted that this process is a function of three main mechanisms: interception, sedimentation, and Brownian diffusion [12]. Interception occurs when the diameter of the particle is sufficiently large that its streamline carries it directly to the collector surface. When the action of gravity causes contact between particles and collectors that would not have otherwise contacted, this mechanism is referred to as sedimentation. Finally, as all particles are undergoing Brownian motion (or diffusion) on a small scale as they travel along a given streamline, this Brownian diffusion can sometimes cause them to contact the surface of the collector. Brownian diffusion is of particular relevance for smaller particles such as the anthropogenic nanoparticles being considered in this work [12].

The overall efficiency with which a given suspension of particles will contact the surface of a collector can be considered as the sum of the individual contributions of each of these three aforementioned mechanisms. This is commonly referred to as the single-collector contact efficiency and is described by the following expression:

$$\eta_0 = \eta_I + \eta_G + \eta_D \quad \textbf{(1)}$$

where η_0 is the overall single-collector contact efficiency, η_I is the contribution due to interception, η_G is the contribution due to gravity (sedimentation), and η_D is the contribution due to Brownian diffusion [13]. Previous studies have suggested that the three transport mechanisms can be expressed as power functions of the primary dimensionless groups thought to influence the transport of particles to the collector surface [14, 15] (e.g. $\eta_D = aA_S^b N_R^c N_{Pe}^d N_{vdW}^e$, where a-e are constants) [13].

Attempts have been made by several groups to develop semi-empirical correlations that may be used to describe the individual contributions of each of the three

mechanisms to the overall single-collector contact efficiency. For many years, the equation proposed by Rajagopalan and Tien (RT) was the approach most commonly used to determine the single collector contact efficiency for colloid transport in saturated granular media [15]. However, Tufenkji and Elimelech [12] have recently proposed a new correlation equation for predicting the single-collector contact efficiency. This new correlation is quickly gaining widespread acceptance as providing more attention to the fundamental processes governing particle transport and has been shown to provide better agreement with experimental data. Tufenkji and Elimelech developed a method whereby optimal values of the power-law constants for each of the three transport mechanisms could be obtained through regression analysis. The correlation equation proposed by Tufenkji and Elimelech (TE) [12] is given by:

$$\eta_0 = 2.4 A_S^{1/3} N_R^{-0.081} N_{Pe}^{-0.715} N_{vdW}^{0.052} + 0.55 A_S N_R^{1.675} N_A^{0.125} + 0.22 N_R^{-0.24} N_G^{1.11} N_{vdW}^{0.053} \quad \textbf{(2)}$$

where A_S is a porosity dependent parameter of Happel's model ($A_S = 2(1-\gamma^5)/(2-3\gamma+3\gamma^5-2\gamma^6)$), N_R is the aspect ratio, N_{Pe} is the Peclet number, N_{vdW} is the van der Waals number, N_A is the attraction number, and N_G is the gravity number.

Simply making contact with a collector surface does that ensure that a colloid will attach. In fact, particle removal from the pore fluid is often thought of as being the product of the single-collector contact efficiency and the attachment efficiency [13]:

$$\eta = \alpha \eta_0 \quad \textbf{(3)}$$

where α, the attachment efficiency, is the ratio of the rates of particle attachment to particle contact and η is the single-collector *removal* efficiency. The attachment efficiency ranges from 0 (no particle attachment) to 1 (all particles that contact the grain surface are retained). Currently, there are no satisfactory theoretical models to describe the attachment efficiency. The classic model put forth by Derjaguin, Landau, Verwey, and Overbeek (i.e., DLVO theory) attempts to determine a function relating a particle's total interaction potential to the sum of attractive and repulsive forces, hydrodynamic forces and the separation distance between particle and collector [16, 17]. However, experimental evidence does not satisfactorily support predictions made using this model [6-9]. Alternatively, Yao et al. [13] proposed an expression for the attachment efficiency

which they obtained through the integration of a mass balance of particles over a differential volume of the porous media:

$$\alpha = -\frac{2d_c}{3(1-\varepsilon)\eta_0 L}\ln(C/C_0) \quad (4)$$

where d_c is the mean diameter of a collector, L is the length of the column of porous medium, ε is the porosity of the porous medium, C and C_0 are respectively the breakthrough and influent particle concentrations [11]. The concentration value that is considered to be the "breakthrough" value is the average steady state concentration of particles effluent from the column following the initial injection of a colloidal suspension [12]. The influent particle concentration is obtained by directly measuring the particle concentration of the "unfiltered" colloid suspension.

1.3 The Role of Particle Size in Colloid Deposition

As previously discussed, the overall efficiency with which a suspension of particles contacts the surface of a collector can be considered the sum of the individual contributions of interception, sedimentation, and Brownian diffusion. As particle size changes, the contribution of each of these mechanisms to the single-collector contact efficiency also changes. Furthermore, both van der Waals and electrical double layer (EDL) forces have a dependence on particle size which results from the necessity to account for the radii of curvature of the two surfaces in the force calculations [9]. In order to better illustrate the significance of particle size, it is convenient to represent the total interaction potential between the two surfaces as:

$$\phi_T = G(\psi_1, \psi_2, A, \kappa, h)\, F(a) \quad (5)$$

where Φ_T is the total interaction potential between the surfaces and is a product of G (a function of surface potentials, Hamaker constant, Debye length and separation distance) which is highly dependent on the chemistry of solutions and $F(a)$ given by $F(a) = (a_1\, a_2) / (a_1 + a_2)$ for particles of radii a_1 and a_2 and by a_p for a particle interacting with a flat plate [9].

Classical DLVO theory predicts a dramatic increase in the total interaction energy of a colloidal suspension with increasing particle size and subsequently predicts

significant decreases in the attachment efficiency and the rate of coagulation. While this theory is still considered to be the most rigorous treatment of colloidal interactions available, simplifying assumptions (i.e., perfectly smooth and spherical particles/collectors, etc.) involved in its derivation limit its usefulness [16, 17]. Furthermore, a number of colloidal interaction forces (i.e., hydrophobicity, hydration forces, etc.) have been neglected in its derivation and while they may be insignificant at larger separations, their contribution to the total interaction can become significant at short distances [9]. Contrary to the predictions of DLVO theory, a growing body of experimental evidence has found that colloidal stability and attachment efficiency may be independent of particle size [6-8]. Various explanations have been proposed to rationalize this discrepancy such as the surface roughness of the particles or collectors, hydrodynamic interactions, the non-homogeneity of surface charge distribution, the dynamics of colloidal interactions and coagulation/deposition in the secondary energy minimum [9]. While each of these factors likely merit attention, the current understanding of these factors precludes their inclusion in any rigorous quantitative assessment.

1.4 The Role of Natural Organic Matter in Colloid Deposition

The interactions between various contaminants and subsurface sediment grains have been found to be highly dependent on the physicochemical and hydrodynamic conditions that are predominant in the subsurface environment [18-21]. As this is likely to be true for anthropogenic nanomaterials, it is important to ensure that any laboratory scale experiments designed to model the transport and fate of contaminants in the subsurface are representative of the system that they are modelling. One environmental factor that is often not accounted for in transport studies is the presence of organic macromolecules in groundwater. This natural organic matter (NOM) is ubiquitous in natural systems and cursory examination of works related to NOM indicates that it is likely to have a significant impact upon the surface potential of colloidal particles [22, 23] and influence the dynamics of colloidal transport in subsurface systems [19, 22-26].

The term "natural organic matter" is a collective term for a group of organic macromolecules found in both subsurface and surface waters that range in composition

from complex residues of cell wall structures to polysaccharides, proteins and organic acids such as humics and fulvics. These macromolecules are formed through the decomposition of plant, animal and bacterial tissue and the relative contributions of these components to the natural organic matter present in a particular area is influenced by the area's physical, geochemical and hydrological characteristics as well as fluctuating factors such as temperature, sunlight and biological prevalence [27].

While it is recognized that these ubiquitous macromolecules have an important effect on soil and aquatic systems due to their role in buffering pH and in increasing the cation exchange capacity, their influence on the stability of colloidal suspensions is largely uncertain. One particular fraction of NOM known as humic acid (HA) has been selected as the particular focus of this investigation. They are natural polyelectrolytes and are considered to be organic acids despite having a wide variety of functional groups. *In-situ* microscopic examinations of HAs have found that their macromolecular structure is not only highly dependent upon solution chemistry due to the protonation/deprotonation of their various functional groups but also upon their origin (soil versus fluvial). Some notable differences commonly observed between the macromolecular structures of HAs of different origin are the lower solubility, higher aromatic content and lower carboxyl content of soil derived HAs relative to fluvial humics [28]. HAs form more than one type of macromolecular structure in aqueous suspensions that is not so simply characterized as to say that HAs form rings in acidic and high ionic strength solutions and elongated structures in dilute or alkaline solutions as was previously held [29]. Although there has been a great deal of study of natural organic matter, little is known about its impact on the stability of nanoparticle suspensions.

1.5 Objectives

The general objective of this investigation is to determine the effect of particle size in conjunction with that of the presence of NOM on the transport of nanomaterials under saturated conditions representative of groundwater environments. The specific objectives of this study are (i) to perform an investigation of the effect of colloid size on the transport and fate of nanoparticles in a model groundwater system under a broad range of

physicochemical conditions; (ii) to investigate whether the presence of NOM would similarly impact the transport and fate of nanoparticles as they do that of micron-scale colloids; and (iii) to characterize the materials used in the investigation aimed at aiding in the interpretation of data obtained from filtration studies.

2.0 Theory

2.1 Material Characterization

2.1.1 Particle Sizing

One of the aims of this project was to develop a better understanding of the role that particle size plays in colloid transport in aquatic systems. According to the DLVO theory, particle transport should be significantly influenced by particle size. As particle size increases, the presence of heightened energy barriers should greatly increase the stability of a colloidal suspension. In order to accurately assess the impact that particle size has on transport, it is necessary to first measure the size of the particles used during the experimental investigation and to this end, size measurements were carried out using a technique known as Dynamic Light Scattering (DLS). The theory behind this technique will now be discussed in detail.

As particles are suspended in a medium, they are constantly undergoing collisions with solvent molecules and neighbouring particles and as a result they undergo random (Brownian) motion. Due to the random nature of this "walk" the motion of a particle undergoing Brownian diffusion is not measured as a velocity but rather by its translational diffusion coefficient (D). The Einstein relation on kinetic theory states:

$$D = \mu k_B T \tag{6}$$

where μ is the mobility of the particles, k_B is Boltzmann's constant and T is the temperature. This relationship shows that diffusion is directly proportional to temperature [30]. At low Reynolds numbers (i.e. laminar flow regime), Stokes law states:

$$\frac{1}{\mu} = 6 \pi \eta a_p \tag{7}$$

where η is the viscosity and a_p is the particle radius. Combining and solving for the hydraulic diameter of the particle (d_H) results in the well known Stokes-Einstein equation:

$$d_H = \frac{k_B T}{3 \pi \eta D} \tag{8}$$

an examination of which demonstrates that the rate of Brownian diffusion is inversely proportional to the hydraulic diameter of the particle.

Measurements of particle size can be obtained using DLS. Fundamental to this process is the fact that as light hits small particles the light is scattered. The Rayleigh approximation states that $I \propto d^6$ where I is the intensity of scattered light [31]. When many beams of light are scattered by many small particles, the beams interfere with each other resulting in a complex and dynamic speckle pattern. The rate at which the intensity pattern changes with time can be related to the size of the particles. If the particles are small, they will move rapidly and their intensity fluctuations will be faster while conversely, larger particles will move less rapidly and their intensity variations will be slower [32]. For monodisperse particles, a correlation equation can be used to plot the intensity variation versus time:

$$< I(t)\, I(t+\tau) > = G(\tau) = A\,[1 + B \exp(-2\, D\, ((4 \pi n / \lambda) \sin(\Theta / 2))^2\, \tau)] \tag{9}$$

where A is the baseline correlation function, B is the intercept of the correlation function, D is the diffusion coefficient, n is the refractive index of the solution, λ is the wavelength of the laser, θ is the scattering angle, t is time and τ is the time difference (i.e. sample time) of the correlator [32]. The mean diameter (z-average) and the width of the distribution (polydispersity) are then calculated from the values of the correlation equation versus time, often using the cumulants analysis as described in ISO 13321 which states that a third order polynomial can be used such that:

$$\ln(G_1) = a + b\tau + c\,\tau^2 \tag{10}$$

where b is the z-average diffusion coefficient and $2\,c / b^2$ is the polydispersity index [32].

2.1.2 Zeta Potential

DLVO theory predicts that the total interaction energy between particles in a colloidal suspension is dependent upon a number of factors, including surface potential. As previously mentioned, it is predicted that particle size and the presence of NOM will have significant impacts on the surface potential of a suspension of colloids. To determine whether the behaviour of suspensions during filtration experiments can be explained by these changes in surface potential, it is necessary to characterize the surface potential of the colloids across the range of experimental conditions investigated. Since direct measurement of the surface potential of a colloidal particle is difficult, indirect measurements of surface potential are often used in their stead and one such measure is known as the zeta potential. Zeta potential can be determined by making use of a process known as Laser Doppler Velocimetry (LDV) in conjunction with Phase Analysis Light Scattering (PALS) [33]. The rationale behind these measurements as well as a detailed description of the theory behind this technique is provided below.

The majority of particles in an aqueous suspension carry a charge on their surface. This surface charge is largely the result of the ionization of acidic and basic functional groups on the particle surface. The dissociation of an acidic functional group results in a negatively charged surface whereas the ionization of a basic group will lead to the formation of a positively charged surface. The net surface charge of a particle is then a function of the relative strengths of its various acidic and basic functional groups and of the pH of the solution. The development of a net charge at the surface of the particle affects the local distribution of ions and leads to the development of a boundary layer wherein there exists a higher concentration of counter ions than that of the bulk phase. This boundary layer can be further subdivided into two regions depending upon how strongly the counter ions in these regions are associated with the surface of the particle. The inner region is known as the Stern layer and within this region ions are very strongly associated with the surface whereas the ions in the outer region, known as the diffuse layer, are much less firmly associated [16, 17]. Furthermore, within this diffuse layer there exists a notional boundary wherein the ions inside that boundary remain associated with the particle as it travels through the medium. This boundary acts as the surface of

hydrodynamic shear for the particles and the electrical potential at this boundary is known as the zeta potential.

An important property of charged particles is their tendency to interact with an applied electric field. These interactions are collectively referred to as electrokinetic effects and of interest in this discussion is the effect known as electrophoresis. As charged particles suspended in an electrolyte are subjected to an applied electric field, they will have a tendency to be attracted to the oppositely charged electrode. The velocity of a particle in an electric field is called its *electrophoretic mobility* and can be related to the zeta potential of a particle through use of the Henry equation [34]:

$$U_\varepsilon = \frac{2\,\varepsilon z\, f(\kappa a_p)}{3\eta} \tag{11}$$

where U_ε = electrophoretic mobility, ε = dielectric constant of the solution, z = zeta potential, and $f(\kappa a_p)$ is the Henry's function (dependent upon κ = Debye length and a_p = particle radius). The reciprocal of the Debye length is often thought of as being the "thickness" of the electrical double layer. Well known approximations are often used when determining the appropriate value of the Henry's function. For the common case of particles larger than 0.2 microns dispersed in more than 10^{-3} molar 1:1 electrolyte, the Smoluchowski approximation is used and the Henry's function is taken as 1.5. For small particles in the presence of less than 10^{-3} molar 1:1 electrolyte, the Huckel approximation is used and 1.0 is used for the Henry's function [34]. In other words, when the thickness of the electrical double layer is small relative to the size of the particle the Smoluchowski approximation is used and when particle size is small relative to the EDL thickness, the Huckel approximation is used. Alternately, the Debye length κ can be calculated using:

$$\kappa^{-1} = \left(\frac{\varepsilon_0\, \varepsilon_r\, k_B\, T}{2000\, I\, N_A\, e^2} \right)^{0.5} \tag{12}$$

where ε_0 is the permittivity of free space (F/m), ε_r is the relative permittivity of the medium, I is the ionic strength of the medium (mol/L), N_A is Avogadro's number and e is the electronic charge (C) [33].

The measurement of electrophoretic mobility using a Malvern Instruments Zetasizer Nano makes use of a combination of Laser Doppler Velocimetry (LDV) and

Phase Analysis Light Scattering (PALS) and is known as the M3-PALS technique [33]. Light scattered from a moving particle causes a shift in the frequency of that light. When combined with a reference sample having a similar path length, interference results in a modulated beam having a beat frequency equal to the difference between sample and reference beams. This beat frequency can then be compared to a reference frequency and used to determine the magnitude of the Doppler shift [33]. Measurements of electrophoretic mobility in a closed capillary are often complicated by a phenomenon known as electroosmotic flow wherein fluids directly adjacent to the capillary walls begin flowing. Traditionally, this complication was avoided by taking measurements at the stationary layer but difficulties in accurately determining the thickness of the stationary layer led to large inaccuracies in mobility measurements, particularly if the cell wall was highly charged [33]. Recently, investigations into the relaxation times pertinent in electrophoresis and electroosmosis have shown that colloidal particles respond to an applied field considerably faster than does the bulk fluid in the capillary [35]. An important implication of this research is that it is possible to alternate the electrical current at such a frequency that electroosmosis is suppressed while colloidal particles are still able to follow the field according to their DC mobility. In modern electrophoresis techniques such as the Mixed Mode Measurement or M3-PALS technique used by the Zetasizer Nano, this principle is further developed as the electric current is alternated using both Fast Field Reversal (FFR) and Slow Field Reversal (SFR) and the difference between the mean of the two is used to determine both the mobility contribution of electroosmotic flow and the charge of the capillary walls [33].

3.0 Materials and Methods

3.1 Materials' Selection and Preparation

3.1.1 Nanoparticles

Sulphate Latex Microspheres: Latex microspheres are a classic example of model colloids as they can be obtained with a wide range of functional groups and well-defined surface properties. Sulphate latex microspheres of varying sizes (50 nm, 110 nm, and 1500 nm) and mass concentrations were purchased from Interfacial Dynamics

Corporation. These particular particles were selected for investigation because they range in size from nano-scale to micron-scale while having surface charge densities that are reported to be comparable. Their sizes, electrophoretic mobilities and relative hydrophobicities have been measured and analyzed.

Solutions used in colloid filtration experiments were prepared in 100 mL volumetric flasks by diluting stock colloidal samples in electrolyte of varying ionic strength (1 – 100 mM KCl). The ionic strength of the electrolyte was varied through the addition of a 1 M KCl stock solution to deionized (DI) MilliQ water. Number concentrations of the differing sized particles were chosen in order to provide maximum resolution in a UV-visible spectrophotometer. The number concentrations used for the 50 nm, 110 nm and 1500 nm latex colloids were respectively, 1.15×10^{11}, 1.16×10^{10} and 8.04×10^{6} particles/mL. For all experiments, pH was maintained at 5.7±0.2.

3.1.2 Collectors

Ultrahigh Purity Quartz Sand: Selected for use as a model collector, this ultrahigh purity sand, though not perfectly representative of natural soils, was selected to provide a closer approximation to natural systems than traditionally examined media (such as soda-lime glass beads). The average grain size of the purchased sand (Sigma-Aldrich) was 0.2 – 0.4 mm, but prior to use, the sand was sieved using -50/+70 U.S. standard sieves (300 and 212 μm. mesh size, respectively) to obtain a sand sample having an average grain size of 256 μm. Given the very small scale of the particles being examined, it is essential that all sand media being used be of the utmost purity and cleanliness. To ensure cleanliness of the media being used in the experiments, all media was cleaned according to the procedure outlined by Litton and Olson [36]. This process involves first bathing the media in 12 M HCl for twenty-four hours, and then washing with DI water until the pH of the rinse solution reaches 5.5-6.0. The media was then baked in a MAS 7000 Microwave Furnace at 120°C for one hour and then at 800°C for five hours. This process is designed to ensure that the media is not only dry but that any organics that may have been present are volatilized.

3.1.3 Natural Organic Matter (NOM)

A well-characterized form of NOM (Suwannee River Humic Acid (SRHA)) was obtained from the International Humic Substances Society (IHSS). Experiments were performed using solutions containing NOM at ionic strengths and pHs that are considered to be representative of groundwater conditions. Collectively, natural organic matter (NOM) represent a significant fraction of organic carbon present in soil and aquatic systems [28] and its concentration as humic substances is found to range between 0.5 – 5 mg/L in streams, rivers and lakes, between 10 – 30 mg/L in marshes, bogs and swamps [37] and between 1 – 50 mg/L in groundwater systems [38].

Stock humic acid solutions were prepared using 100 mg vials of dry SRHA purchased from the IHSS. Dried SRHA was dissolved in DI containing 1 mM NaOH to ensure complete dissolution. Since humic acids are generally the second most plentiful fraction of humic substances (following fulvic acids) [37], a moderate humic acid concentration of 5 mg/L was selected for experiments. Electrolytes for experiments in the presence of humic acids were prepared using appropriate volumes of humic acids buffered to a pH of 5.7±0.2 using appropriate volumes of 0.1 M NaOH.

3.2 Colloid Filtration Studies

To examine the macro-scale deposition of the selected anthropogenic nanomaterials onto quartz surfaces, real time measurements of the transport and deposition of these nanomaterials have been made as a suspension of these particles travels through a fully saturated column packed with granular media. The transport and deposition of nanoparticles occurring within the column is quantified on-line using a UV-Vis spectrophotometer (Agilent Technologies) by measuring the difference between the light absorbed by the column influent and effluent solutions. The environmental parameters (i.e., ionic strength and NOM concentration) affecting the deposition of colloids onto collectors has been systematically examined in order to determine their individual effects.

Because the purpose of this study is to examine the interaction between colloidal particles and granular collectors under saturated conditions, it is essential that extreme care be given to remove all air from the system to prevent the formation of microscopic air bubbles which could affect the observed colloid deposition. To this end, preparation

for a column filtration experiment has involved the preconditioning of all media to be used in an experiment by soaking it in the electrolyte solution to be used in the experiment. Volumetric flasks (100 mL) containing the solutions and media were left in a shaker for a period of 24 hrs prior to each experiment.

To maximize the reproducibility of the column experiments, a meticulous and rigorous column packing procedure has been developed. First, a fine nylon mesh membrane is placed at the bottom of the column to ensure that none of the collectors (sand grains) exit the column. If the collectors should happen to exit the column, then they could either clog the line effluent from the column or they could make their way into the measurement cell and affect the absorbance readings. In order to ensure that the column was packed identically each time, the column was gently vibrated throughout the addition of the media to the column. This has ideally allowed the media to pack together just as tightly in each experiment. The diameter of the packed column was 10 mm and its length varied between 150 and 165 mm. A schematic diagram of the experimental setup has been included for illustrative purposes and is given in Figure 1.

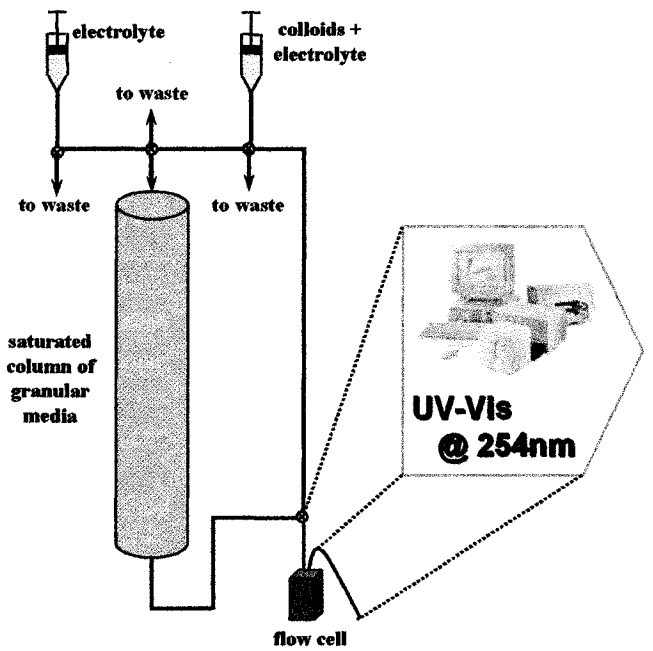

Figure 1. Schematic diagram of experimental setup

Finally, once the column was packed and before the introduction of the colloids to the system, at least twenty pore volumes of electrolyte solution was passed through the column to ensure that the column was fully equilibrated with the background solution (one pore volume is the volume of free-space in the column unoccupied by media). This was in accordance with the equilibration protocol established by Tufenkji and Elimelech [39].

The experiment itself then consisted of injecting approximately three pore-volumes of the colloid solution through the fully equilibrated column at an approach velocity of approximately 2.1×10^{-4} m/s. The deposition of this colloidal suspension was then monitored using a UV-Vis spectrophotometer at a wavelength of 254 nm and using a 1-cm flow-through cell. Through observation of the difference between the absorbance of the colloid solutions influent and effluent from the column, it was possible to determine how much of the influent colloid solution deposited on the surface of the collectors.

3.3 Material Characterization

To assist in the interpretation of data obtained from colloid filtration experiments, it is necessary to characterize the physicochemical characteristics of the materials being used in the experiments in question. This characterization includes the determination of particle size through dynamic light scattering (DLS) and the surface charge of the colloids through mobility measurements. The procedures used for each of these characterization techniques are outlined in further detail below.

3.3.1 Particle Sizing

Particle size measurements were made for each of the samples prepared for colloid filtration experiments using disposable capillary cells (Malvern). For the size measurements obtained using DLS to be accurate it is essential that the motion of particles in the dispersion be truly random. This means that all samples being measured must have achieved thermal stability in order to eliminate natural convection.

3.3.2 Zeta Potential

Measurements were made for each of the samples prepared for colloid filtration experiments using disposable capillary cells. Zeta potential instruments are not calibrated but rather they use first principles in their measurement protocols. Due to the consumable nature of the disposable capillary cells, the performance of these cells deteriorates with time. As such it is essential that all cells be verified before and throughout use by measuring the mobility of a zeta potential standard. The standard provided with the Malvern Instruments Zetasizer Nano is a well characterized dispersion of latex particles (DTS0050) and yields a zeta potential of -50 mV (± 5 mV). Sample mobility is measured by conducting a phase comparison of the detected signal with that of the reference frequency (the modulator frequency of 320 Hz is used as a reference) during the FFR portion of the measurement. The Henry equation (Eq11) is then used to convert mobility measurements to zeta potential. The Smoluchowski approximation is used to convert mobility to zeta potential. The Huckel approximation is only used in cases where EDL thickness is large relative to particle size and this only occurs for the smallest particles at very low ionic strengths and this is not the case in this instance.

4.0 Results and Discussion

4.1 Colloid Filtration Studies

A series of colloid filtration experiments were performed across a broad range of physicochemical conditions and resultant from these experiments is a series of particle breakthrough curves. This data was then interpreted using equations [1, 2 and 3] previously developed. This resulted in the development of a series of attachment efficiency versus ionic strength data for each of the three latex particles studied in both the presence and absence of HAs. This data has been summarized and is presented in Figure 2.

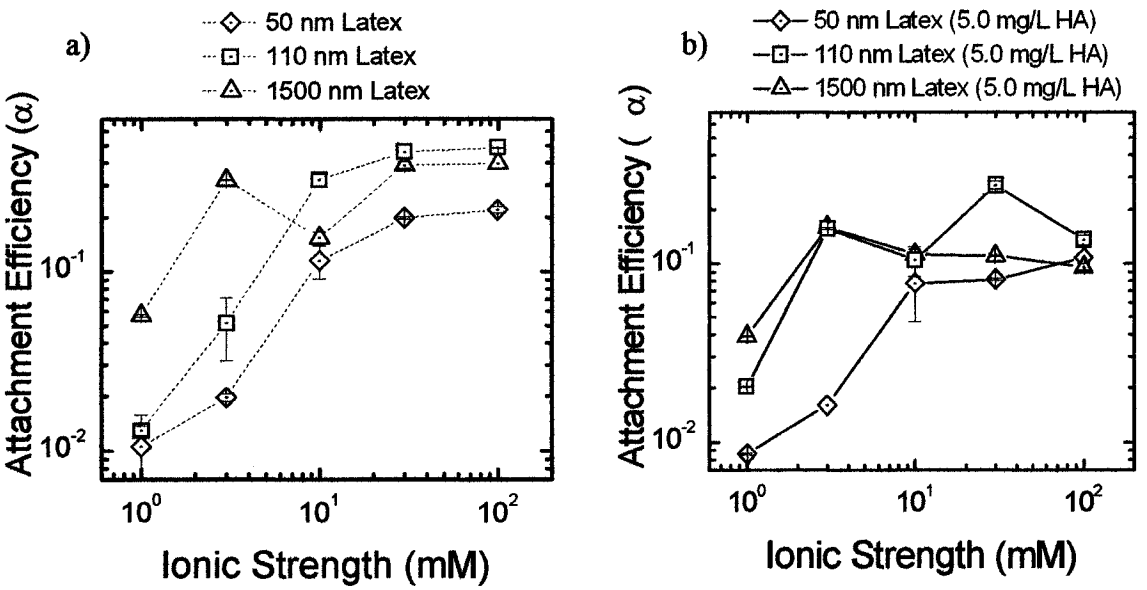

Figure 2. Attachment efficiency versus ionic strength

4.1.1 The Effect of Particle Size

Inspection of Figure 2 reveals insight into the transport and filtration behaviour of the three different-sized model colloids across the range of physicochemical conditions studied. Focusing first on the pattern observed for each of the particles, it can be noted that as ionic strength of the electrolyte was increased, attachment efficiency generally increased for all particles examined. Upon first inspection this finding seems theoretically consistent as it is expected that the thickness of a particles' EDL should decrease as ionic strength is increased. As a result, the energy barriers that are encountered during particle-grain surface interactions are expected to be smaller resulting in increased attachment of particles on the grain surface.

Examination of Figure 2 also reveals a trend in measured values of the attachment efficiency with increasing particle size. At very low ionic strengths, it can be observed that there is an increase in the attachment efficiency with increasing particle size which is in marked contrast with DLVO theory that predicts a decrease in attachment efficiency with increasing particle size. This observation will be discussed in greater detail in section 4.2.2.1.

As ionic strength is increased, a transition in the behaviour can be observed. While at low ionic strengths (1 – 10 mM KCl) there is a marked increase in attachment efficiency with changing ionic strength, at higher ionic strengths (10 – 100 mM KCl), the effect on attachment efficiency is lessened. Furthermore, the effect of particle size on attachment efficiency is no longer observed at high ionic strengths with all three particle sizes reaching plateaus in their attachment efficiencies in approximately the same range (0.3 ± 0.2).

To interpret the trends observed between the particle sizes and to rationalize some of the apparent contradictions of DLVO theory, it is necessary to have a more thorough discussion of the role of particle size in DLVO theory. Due to their usefulness in data interpretation, equations will be presented that will allow the development of quantitative estimates of the potentials and energy barriers involved in the colloidal interactions being examined. As previously discussed, classic DLVO theory states that the total interaction potential between two surfaces should be the sum of attractive van der Waals and repulsive EDL interactions as represented by:

$$\phi_T = \phi_V + \phi_E \tag{13}$$

where Φ_T is the total interaction potential, Φ_V is the vdW interaction energy and Φ_E is the electrostatic repulsion energy. Theoretical expressions for vdW interactions should account for the effect of retardation and one such model proposed by Gregory [40] for the sphere-plate case is given by:

$$\phi_V = \frac{A\, a_p}{6h\left(1+14h/\lambda\right)} \tag{14}$$

where A is the Hamaker constant for the interacting media (Hamaker constant of $1\text{x}10^{-20}$ J was selected for the polystyrene – quartz – water system), h is the separation distance between particle and collector and λ is the "characteristic wavelength" of the interaction, often assumed to be 100 nm [9]. Theoretical expressions for the EDL interaction force have been derived for the cases of constant potential [41], constant charge [8], and intermediate interactions [42]. For the constant potential case, the expression proposed by Hogg, Healy and Fuerstenau (HHF) is given by [41]:

$$\phi_E = \pi\,\varepsilon_0\,\varepsilon_r\,a_p\left(2\psi_1\,\psi_2\ln\left(\frac{1+\exp(-\kappa h)}{1-\exp(-\kappa h)}\right)+\left(\psi_1^{\,2}+\psi_2^{\,2}\right)\ln\left(1-\exp(-2\kappa h)\right)\right) \quad \textbf{(15)}$$

where ψ_1 and ψ_2 are respectively the surface potentials of the colloids and the collectors. While each of these theoretical expressions has their limitations and neither of these "static" models of surface potential can be perfectly representative of reality, the HHF model was selected because it predicts the lowest values of EDL interaction potential [9].

To make use of these theoretical expressions to estimate the energy barriers involved in the particle-surface interactions examined, it is necessary to first have a measure of the surface potentials for the colloidal suspensions examined. As direct measurement of the surface potentials of a suspension of colloidal particles is difficult, an indirect means of measurement was used. The results of this investigation are summarized in section 4.2.2 and a discussion of how these findings may be used in the interpretation of the observed trends of attachment efficiency with increasing particle size and ionic strength is included.

4.1.1 The Effect of NOM

To assist in the interpretation of the data obtained from the colloid filtration experiments and to better highlight the impact of HAs on attachment efficiency with increasing particle size and ionic strength, the data has been rearranged and is presented in Figure 3.

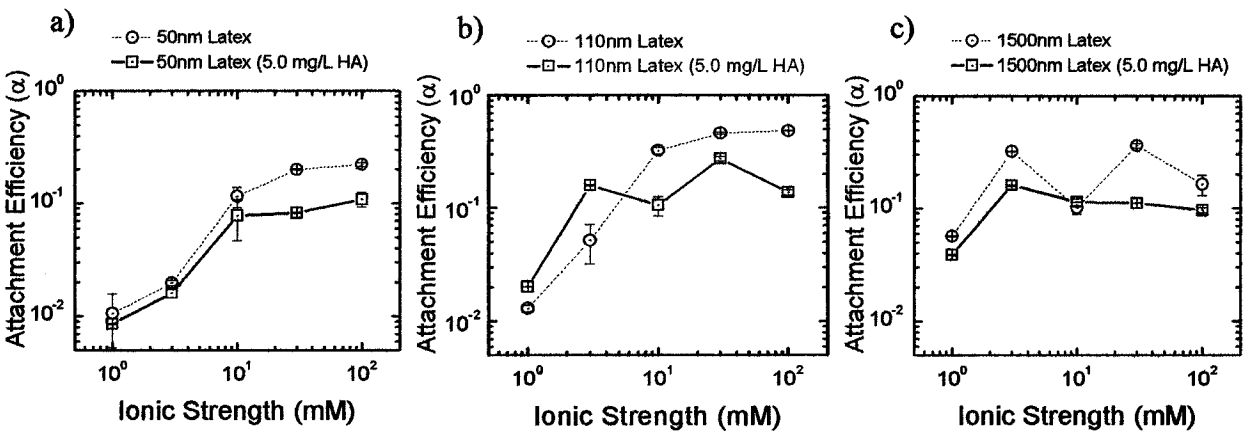

Figure 3. Attachment efficiency versus ionic strength

Examination of these figures shows that presence of HAs generally resulted in a decrease in the observed attachment efficiency for all three particle sizes. To better understand this observation, further discussion of the role of NOM in aquatic systems is required.

It has come to be accepted by many researchers that the primary physicochemical effect of NOM in aquatic systems is that it tends to impart a negative surface charge to suspended particulates and that this increased surface charge should result in an increase in the stability of a colloidal suspension [38]. This finding has been confirmed and supported by the works of many [27, 43, 44]. However, it has also alternately been observed that the presence of larger natural organic macromolecules resulted in the formation of colloidal bridges and resulted in the destabilization and eventual coagulation of a colloidal suspension [27].

To formulate an explanation of the observed decreased attachment efficiency in the presence of HAs for all three particle sizes, it was attempted to determine whether it was a physical phenomenon or a physicochemical effect. A set of experiments were carried out to characterize the colloidal suspensions in the presence and absence of NOM and the results of these experiments and a discussion of how they may be used in the interpretation of the observed data is included in section 4.2.

4.2 Material Characterization

A series of experiments were performed to characterize the materials used in the investigation to aid in the interpretation of data obtained from the filtration studies. These experiments include the measurement of particle size through dynamic light scattering and the characterization of surface potential through mobility measurements. These results and a discussion of how they can aid in the interpretation of colloid filtration experiments are presented in detail.

4.2.1 Particle Sizing

Differences in particle size in the presence and absence of HAs may have contributed to the impact of HAs that was observed during colloid filtration experiments. In order to determine the role HAs may have played in decreasing the attachment efficiency of all

three particle sizes, it was important to measure the size of the actual samples used during experiments. Furthermore, this also allowed for the confirmation that the measured size of the particles corresponds with the size quoted by the manufacturer and provided a means of observing whether particle coagulation or flocculation was occurring. The results of these particle size measurements have been summarized and are presented in Figure 4.

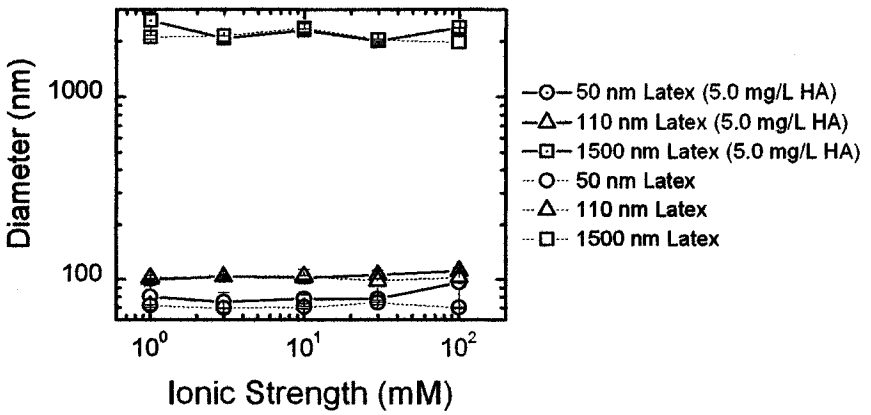

Figure 4. Hydraulic diameter versus ionic strength

Observation of the results presented in Figure 4 lends itself to several insights. While some slight deviation between the measured hydrodynamic diameter of the particles and the size quoted by the manufacturer may be observed, it can be concluded that the hydrodynamic diameter was unchanged in the presence of NOM. This observation tends to indicate that a physical mechanism is not responsible for the decrease in the attachment efficiency for all three particles that was observed in the presence of HAs and that a physicochemical mechanism bears further consideration. Specifically, the hypothesis that in the absence of NOM increased physical straining of larger particles led to increased particle removal is disproved.

4.2.2 Zeta Potential

To interpret the role that surface potential may play in the attachment of the different sized particles over the range of conditions examined, mobility measurements were made with all three latex particles in the presence and absence of HAs and the data obtained from these experiments is presented in Figure 5.

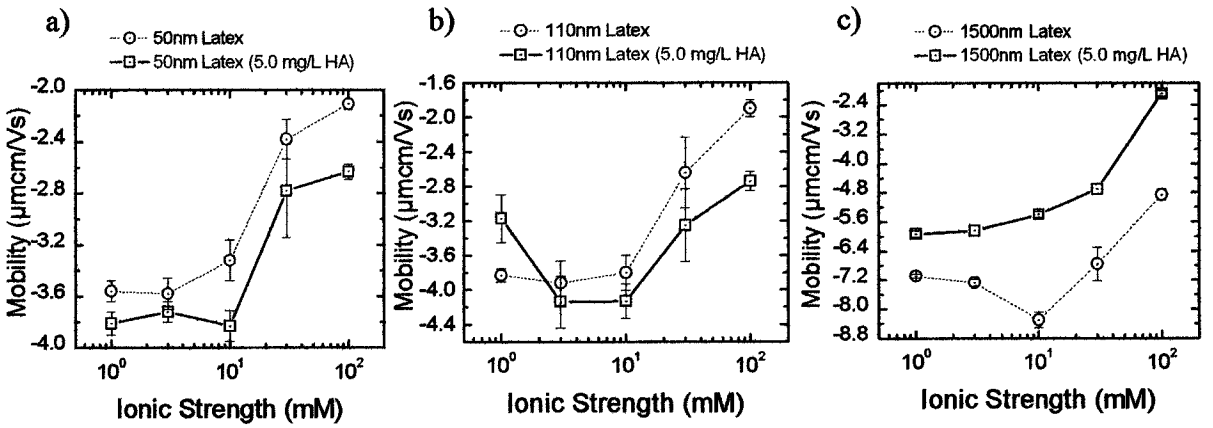

Figure 5. Electrophoretic mobility versus ionic strength

As previously discussed, measured mobility data is often converted to zeta potential (Eq11) as it is commonly used as an interpretive tool. Resultant from these conversions is a series of zeta potential versus ionic strength data and this data has been summarized and is presented in Figure 6.

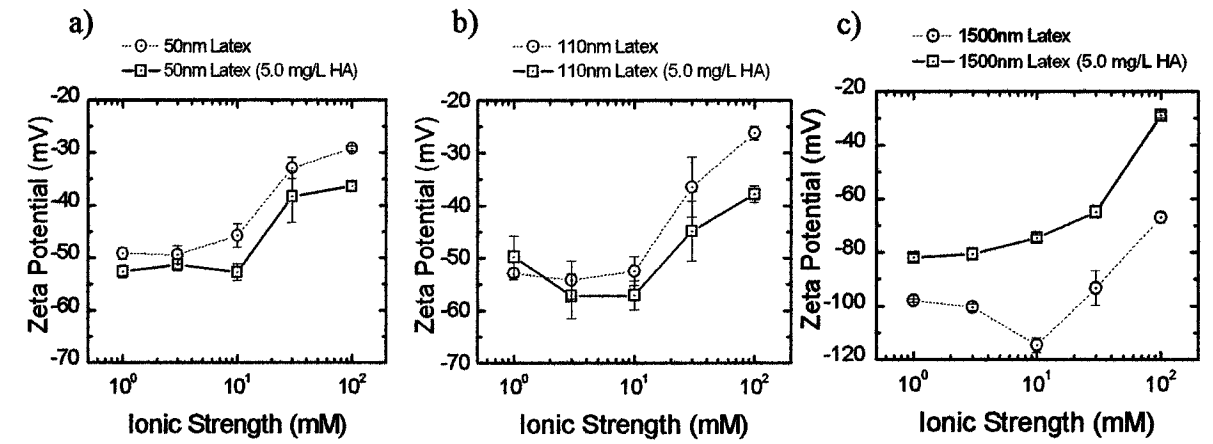

Figure 6. Zeta potential versus ionic strength

The electrical charge and potential of latex particles originates from the dissociation of functionalized surface groups. As these groups are successively protonated or deprotonated with changes in pH, the surface charge of the particle changes. In the EDL model, charged surfaces in an aqueous solution will attract counter-ions from the solution. The presence of these counter-ions "masks" the charge on the

particle's surface. At a given pH and as the ionic strength of the solution is increased, there will be more counter-ions present in solution. The particles' electrical double layer will then "shrink" as the ionic strength of the solution is increased and result in a continuous decrease in measured potential [5]. However, rather than continuously decreasing with increasing ionic strength, the general shape of the three pairs of experimental mobility and zeta potential curves exhibit a maximum at a moderate ionic strength (10 mM KCl) which is in contrast to what may be predicted by the DLVO theory.

This finding has been observed by a number of groups and various qualitative explanations for this behaviour have been proposed including the preferential adsorption model and the so-called hairy layer model [5, 45-48]. The preferential adsorption model argues that this maximum may be explained by the preferential adsorption of co-ions onto the surfaces of latex particles amplifying the electrokinetic potential of the colloids [47]. The hairy layer model envisions the surface of polymer lattices as being comprised of polyelectrolyte chains carrying the surface charge [45, 46]. As ionic strength is varied, this layer is hypothesized to expand and contract due to the repulsion of the functional groups. As this occurs, the location of the plane of shear is said to be affected and consequently so too is the electrokinetic potential. Elimelech and O'Melia [5] considered both of these models and while they do not argue against the existence of a hairy layer at the surface of latex particles, they concluded that the maximum that often occurs in the mobility curves of negatively charged polystyrene latex particles is more likely to be determined by the combined action of co-ions and counterions at the interface [5]. They proposed that the shape of latex particles' mobility curve as a function of electrolyte concentration is determined by the relative contributions of three competing processes: (1) Neutralization of negative charge on the surface by adsorption of counterions causing a decrease in the electrokinetic potential (less negative); (2) Approach of co-ions close to the surface of the particles, causing an increase of the electrokinetic potential (more negative); (3) Compression of the diffuse double layer due to high bulk concentration of electrolyte, causing a decrease in electrokinetic potential (less negative) [5].

4.2.2.1 The Effect of Particle Size

As was previously discussed, an increase in the attachment efficiency with increasing particle size was observed during the course of colloid filtration experiments, which is in marked contrast with theory. A growing body of experimental evidence does not fully substantiate DLVO theory and the effect of particle size on colloidal stability and attachment efficiency may not be as readily included in rigorous quantitative analysis as current theory espouses [6-8]. Many of the explanations put forth to rationalize these discrepancies merit further attention but certain fundamental processes in colloidal interactions are not yet sufficiently understood to permit their inclusion into the theoretical framework. While it may not yet be feasible to rigorously include these factors in a quantitative analysis, a qualitative discussion of surface roughness, hydrodynamic interactions, surface charge heterogeneities, the dynamics of colloidal interactions and deposition in the secondary energy minimum can be of use in understanding the deviations of observations from the behaviour predicted by DLVO theory. A qualitative discussion of each of these possible explanations will be presented in brief as very thorough discussions of these explanations have been presented elsewhere [49].

1. **Hydrodynamic Interaction**. The hydrodynamic or viscous interaction between two particles or a particle and a surface is a phenomenon caused by the resistance to flow of the liquid in the narrowing gap between the two surfaces. Attempts have been made to include the hydrodynamic resistance into calculations of the theoretical collision efficiency and they have shown that the impact is relatively small [14, 50]. In fact, it has been demonstrated that the hydrodynamic resistance is particularly small for Brownian particles relative to that experienced by larger particles [14, 50]. This means that if the hydrodynamic resistance were included in calculations of the theoretical collision efficiency, suspensions of larger particles should be even further stabilized and as a result, hydrodynamic resistance can not be used to explain the deviations from DLVO theory that were observed.

2. **Dynamics of Interaction**. As was previously discussed, theoretical expressions for the EDL interaction force are generally derived upon an assumption of either constant potential [41], constant charge [8] or an intermediate case based which makes use of the linear superposition approximation [42]. While each of these approximations has its relative merits and applicability, neither of these "static" approximations can be truly representative of the dynamic processes that are believed to be involved in colloidal interactions. While no theory currently exists which rigorously treats the dynamics of colloidal interactions, preliminary investigations into interfacial electrodynamics indicate that hydrodynamic drag on the electrical double layer combined with the fluxes of various ions at the interface might counteract the impact of particle size that is traditionally predicted by DLVO theory and might help to explain some of the deviations from theory that were observed during this investigation [9, 51-53].

3. **Surface Charge Distribution**. Calculations of the theoretical collision efficiency assume that the surface potentials of particles and collectors are both uniformly distributed and constant [41] for a given solution chemistry, whereas examination of mobility measurements indicates that there is likely a distribution of surface potentials within a given suspension. By considering the surface potentials of particles and collectors as random variables, groups have investigated the impact of a distribution of particle surface properties [54] and zeta potentials [55] on coagulation rates and the impact of distributions in zeta potential on deposition rates for both non-Brownian [56] and Brownian particles [9]. Assuming a normal distribution of zeta potentials for their suspensions, Elimelech and O'Melia [9] concluded that a distribution in zeta potentials could not explain the insensitivity to particle size that they observed during deposition studies. Given this conclusion and the fact that an even greater deviation from the results predicted by DLVO was observed during the experiments outlined in section 3.2, it can be concluded that the deviations from DLVO theory that were observed during the colloid filtration experiments can not be explained by a distribution in the surface charge of particles or collectors.

4. **Deposition in Secondary Minima**. When plotting interaction energy versus separation distance, DLVO theory predicts the presence of both a deep energy well (known as the primary minimum) very close to the collector surface and a shallower energy well (the secondary minimum) separated by an energy barrier that impedes deposition in the primary minimum [8]. For a given set of chemical conditions, DLVO theory predicts that both the height of the energy barrier and the depth of the secondary energy well will increase with increasing particle size. Wiese and Healy [8] argued that the apparent failings of predictions made using DLVO theory could be explained using an energetic argument that incorporated the secondary minima. They argued that while heightened energy barriers might decrease the rate of particle coagulation deposition in the primary minimum, the presence of deepening energy wells might lead to the favourable energetic conditions required for deposition in the secondary minimum [8]. Many groups have since reasserted that anomalous particle size effects could be explained by deposition or coagulation in the secondary energy minimum [6, 57]. While the role of the secondary minimum in colloid deposition is still much debated, it is theoretically possible provided that the force resultant from the particle's kinetic energy and the fluid's drag is insufficient to drive the particles out of the secondary minima [9]. Theoretical analysis of the trajectory of Brownian and non-Brownian particles predicts that deposition in the secondary minimum is only possible at the rear stagnation point of a spherical collector where the sum of EDL, vdW and drag forces on the particle are zero [15, 56, 58-60]. This means that while deposition in the secondary minimum is certainly possible, its impact may be limited by the number of available rear stagnation points.

The existence of the secondary energy minimum may be used to explain some of the anomalous particle size effects that were observed during this investigation. Increases in the depth of the secondary energy minimum with increasing particle size could be sufficiently favouring deposition in secondary minima and this could explain the increase in attachment efficiency with increasing particle size. Since the depth of the secondary minimum would increase with increasing ionic strength, it is likely that deposition in secondary minima would be most significant at high ionic strength. This could partially explain the transition in behaviour that was observed with increasing ionic strength. However, the significance of particle deposition in the secondary minimum is still much

debated and since the attachment efficiencies for all three particle sizes plateau in the same range at high ionic strengths, it seems unlikely that deposition in secondary minima alone may explain the observed deviations from predictions.

5. **Surface Roughness**. Calculations of the theoretical collision efficiency assume that both particles and collectors are spherical. While both the particles and collectors selected for this investigation are likely to be considerably more spherical than the majority of those encountered in realistic situations, neither the latex particles nor the sand grains are perfectly spherical. Many groups have investigated the interplay between the effect of particle size and surface roughness on colloidal stability [7, 61, 62] and the disparity with respect to the effect of particle size on deposition that has been observed by a number of groups has been attributed by some to the roughness of the surfaces involved in the interactions [7]. In order to model the impact of surface roughness on the total interaction energy, the roughness of a particle or collector is envisioned as being small half-spheres protruding from their surfaces [9, 57]. Attempts have been made by several groups to develop mathematical models to describe surface roughness in such a way as to account for the relative size of particles and surface asperities [63-65]. While no universally accepted model describing the impact of surface roughness yet exists, initial attempts have been made to model simple interactions wherein the surface asperities of collectors are assumed to be much larger than those of the particles [9]. The results of this investigation showed that the height of the energy barrier was considerably reduced in the presence of these surface asperities. While it was concluded that the presence of surface roughness alone could not account for the observed discrepancies with respect to particle size [9], it was demonstrated that surface roughness could at least be contributing to the observed erroneous particle size effect. It is important to note that the effect of interfacial dynamics or deposition in secondary energy minima that were discussed above may have considerable interplay with the impact of surface roughness. However, the understanding of these factors and particularly of their interplay is still quite limited, and as such, their impact on colloidal stability cannot yet be fully assessed quantitatively [9].

Interaction Energy Profiles

To better understand the observed behaviour, zeta potential measurements were related to surface potential as discussed above and the theoretical expressions for vdW and EDL interaction energy developed previously were used to calculate the heights of the theoretical energy barriers that would exist between colloids and collectors across the range of physicochemical conditions examined in this investigation. As previously discussed, DLVO profiles were calculated by adding the contributions of vdW as given by Gregory [40] and EDL as given by Hogg, Healy and Fuerstenau [41]. The values of zeta potential used for the collectors were taken from Redman et al [66]. The presence of NOM was assumed to not affect the zeta potential of the collectors. This is a reasonable assumption because the crystalline and ultra-pure nature of the collectors should cause them to have very little affinity for the HAs. The results of these computations are summarized in Figure 7.

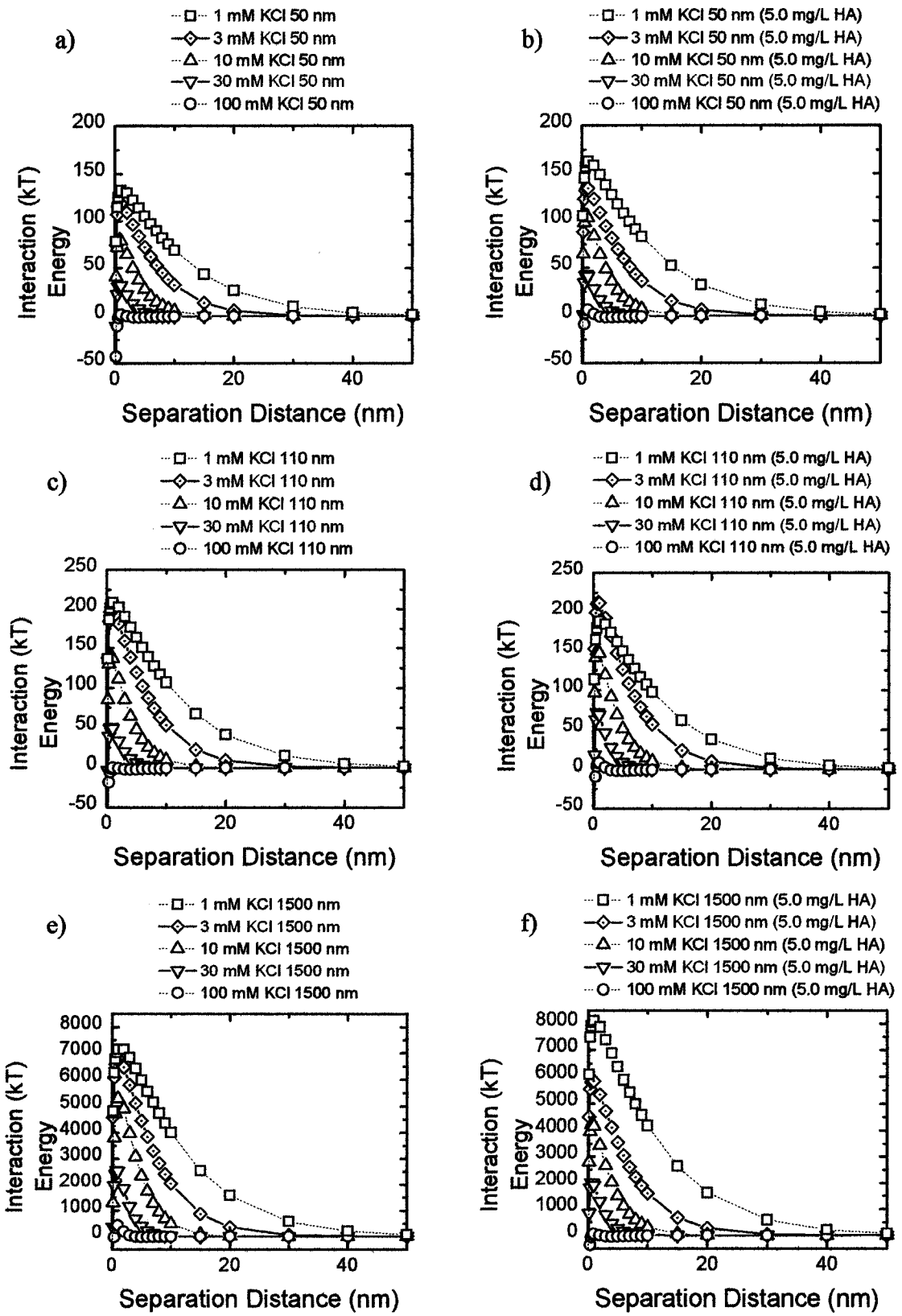

Figure 7: Interaction energy versus separation distance

Examination of these plots shows that the height of the energy barrier is predicted to increase with increasing particle size in both the presence and absence of HAs. This means that if we strictly consider irreversible attachment in the primary energy minimum, the heightening of this energy barrier with increasing particle size should mean that interactions between colloids and collectors should get progressively more unfavourable and in particular, the interactions for the 1500 nm colloids should be highly unfavourable. Given the height of the energy barrier at all but the highest ionic strengths (8050-1995 kT at 1-30 mM), DLVO theory would predict that primary deposition of the 1500 nm colloids should be highly improbable. However, despite these predictions, the reverse trend was observed in this investigation and the attachment efficiency of the 1500 nm colloids is higher than that of either of the two smaller colloids. It should be noted that under these same conditions deposition in the secondary energy well (0.21 - 7.9 kT at 1 - 30 mM, respectively), is more likely than deposition in the primary energy well. Examination of plots of interaction energy versus separation distance serves to highlight the shortcomings of such a simplified and static model for colloidal interactions and reinforces the point that the dynamic nature of colloidal interactions is not fully accounted for in standard DLVO considerations.

4.2.2.2 The Effect of NOM

The presence of HAs leads to an increase in the absolute zeta potential of the suspensions for the 50 nm and 110 nm colloids. As previously discussed, it is accepted by many that NOM's primary physicochemical effect in aquatic systems is to impart a negative surface charge to suspended particulates and that this increased surface charge should result in an increase in the stability of a colloidal suspension [38]. This predicted behaviour is observed in the case of the two smaller nanoparticles. The increases in the absolute values of zeta potential of the colloids observed in Figure 6 should result in increased stability and this has been confirmed by the decrease in attachment efficiencies observed in Figure 3. However, for the 1500 nm colloids, the presence of HAs leads to a decrease in the absolute value of zeta potential as can be observed in Figure 6. Despite this contrary behaviour, observation of the results presented in Figure 3 shows that attachment efficiency was decreased in the presence of NOM, just as it was in the case of the two

smaller nanoparticles. This finding is of great interest because it tends to indicate that surface charge effects can not fully explain the differences in attachment efficiency behaviour that were observed in the presence and absence of NOM for all three particles. In particular, it indicates that that there may be some other mechanisms contributing to the attachment behaviour of the colloidal suspensions (particularly evident for the 1500 nm particles) and that there may be some shortcomings in the ability of DLVO theory to predict colloidal behaviour.

It was the intent of the experimental design to isolate the particle size effect as much as possible by obtaining three colloidal particles of different sizes having similar zeta potentials. Despite this effort, it can be noted that the zeta potential of the 1500 nm colloids was considerably larger than that of the 50 nm and 110 nm particles. As a result, differences that were observed in the attachment efficiency behaviour of the three particle sizes is not purely a particle size effect as had been the intent of the experimental design. While this further complicates the interpretation of the results obtained from the colloid filtration experiments, it has also made possible some other interesting observations about the NOM's interactions that might not have otherwise been observed. Careful inspection of the absolute values of zeta potential for the 50 nm and 110 nm particles relative to those of the 1500 nm particles yielded an explanation for the reversal in charge behaviour that was observed in the presence of HAs for the 1500 nm colloids.

Due to their being preconditioned with HAs as a part of the experimental protocol, it is likely that the HAs would become very closely associated with the hydrophobic surfaces of the latex particles. Since the HAs are likely to bear a particular average surface charge of its own, then rather than amplifying or neutralizing the charge of the particles (as in the model proposed by Elimelech and O'Melia), the HAs could be "masking" the charge of the particles with their own. As was previously mentioned, the average measured zeta potential for the 1500 nm particles was considerably higher than either of the two nanoparticles. It is possible that the average charge borne by the HAs used in these experiments could lie somewhere in between that of the 1500 nm particles and the two nanoparticles. If this is the case, it is possible that the reversal in charge behaviour in the presence of HAs that was observed for the larger colloids can be

explained by the average potential of the HAs lying somewhere in between that of the smaller and larger latex particles.

This does not however, explain why the trend in attachment efficiency for all three particles is the same despite the reversal in charge behaviour that was observed during the zeta potential characterization experiments (for the 1500 nm colloids). While the experimental data obtained throughout the course of this investigation might not provide any conclusive explanations as to why the attachment efficiency trend was seemingly unaffected by the observed reversal in charge behaviour, a partial explanation may be possible. Some of the seemingly erroneous behaviour can potentially be attributed to the influence of some of the short-range forces (e.g., hydrophobic interactions, diffuse-layer interactions, steric interactions) that are often neglected in standard colloidal interactions. For example, the decrease in zeta potential observed for the two smaller particles in the presence of HAs was concluded to be the cause of the decreased attachment efficiency. However, if we alternately concluded that the decrease in attachment efficiency observed in the presence of HAs is the result of some unaccounted-for steric or hydrophobic interaction (for example), it is possible that the presence of the HAs could cause decreased attachment efficiency for all three particle sizes irrespective of the observed reversal in charge behaviour.

5.0 Conclusions

A series of colloid filtration experiments were performed using three different sized latex particles (50 nm, 110 nm and 1500 nm) across a broad range of physicochemical conditions and in both the presence and absence of 5.0 mg/L humic acid. At very low ionic strengths (1 – 10 mM KCl), an increase in attachment efficiency with increasing particle size was observed, which is in contrast with theoretical predictions of decreasing attachment efficiency with increasing particle size. At higher ionic strengths (10 – 100 mM KCl), the effect of particle size on attachment efficiency was no longer observed. Furthermore, the presence of HAs generally resulted in a decrease in the observed attachment efficiency for all three particle sizes. A series of characterization experiments were performed to better understand the observed increased attachment efficiency with

increasing particle size at low ionic strengths and the decreased attachment efficiency in the presence of HAs for all three particle sizes.

While some slight deviation between the measured hydrodynamic diameter of the particles and the size quoted by the manufacturer was observed, it was concluded that the hydrodynamic diameter was unchanged in the absence or presence of HAs and that the results of the deposition studies were not being confounded by the occurrence of particle coagulation. As was previously discussed, an increase in the attachment efficiency with increasing particle size was observed during the course of colloid filtration experiments, which is in marked contrast with theory. It is argued that the apparent deviations from DLVO theory can be explained by interactions between surface roughness, the dynamic nature of colloidal interactions and deposition in secondary energy minima.

The presence of HAs was found to lead to an increase in the absolute zeta potential of the suspensions for the 50 nm and 110 nm colloids, however for the 1500 nm colloids, the presence of HAs lead to a decrease in the absolute value of zeta potential. This finding is of great interest because it tends to indicate that surface charge effects can not fully explain the differences in attachment efficiency behaviour. Careful inspection of the absolute values of zeta potential for the colloidal suspensions yielded the conclusion that since HAs are likely to bear a particular average surface charge of its own, then rather than amplifying or neutralizing the charge of the particles, the HAs could be "masking" the charge of the particles with their own. If the average charge borne by the NOM lies between that of the 1500 nm particles and the two nanoparticles, the reversal in charge behaviour in the presence of HAs can be rationalized.

While the experimental data obtained did not provide any satisfactorily conclusive explanations to the observed attachment efficiencies despite the observed reversal in charge behaviour, a partial explanation may be possible. The seemingly erroneous behaviour could potentially be attributed to some short-range force (e.g., hydrophobic interactions, diffuse-layer interactions, steric interactions) that is often neglected. If we alternately concluded that decreased attachment efficiency in the presence of HAs resulted from some unaccounted-for steric or hydrophobic interaction (for example), then the observed decrease in zeta potential in the presence of HAs could be concluded to be coincidental to the decrease in attachment efficiency rather than causative.

Appendix A: Microsphere Attachment to Hydrocarbons (MATH)

A.1.0 Background and Motivation

Anomalies were observed in the behaviour of the colloidal suspensions in the presence of HAs and since the earlier characterization experiments had not yielded a definitive explanation, it was decided that another possible explanation might lie in some of the short range forces (i.e., London forces, hydrophobicity, etc.) that are not considered in DLVO. In particular, since it is suspected that HAs are closely associated with the hydrophobic surfaces of the latex particles, it was decided to further investigate the hydrophobic interactions between HAs and the particles by characterizing the relative hydrophobicity of the three colloids in their presence and absence. In particular, it is of interest to determine whether the anomalous behaviour of the 1500 nm latex particles can be explained by some difference in the nature of their hydrophobic interactions with HAs.

The process used to manufacture latex polystyrene microspheres is a form of radical polymerization wherein the reactive sites are kept separated from each other by dispersing the monomers in a continuous phase. This process is better known as emulsion polymerization and involves the emulsification of non-polar functionalized styrene monomers in water. Non-polar molecules dispersed in water tend to associate and this is known as the hydrophobic effect. This tendency leads to the formation of nano-scale latex particles that consist of many polymer chains. Despite the presence of repulsive forces due to the surface charge of the particles, if left unchecked polymerization will continue and the size of the resultant latex particles will increase.

To control the production of latex microspheres, surfactants are often used because their hydrophobic tails will tend to be attracted to the polymer surface and the charge of the hydrophilic head repels other similarly coated latex particles. The latex particles used in the present study are surfactant-free. As an alternative stabilizer, many surfactant-free polymerization processes make use of water-soluble polymers and the result is the formation of a "hairy layer" of water-soluble polymer surrounding a hydrophobic polymer core.

Prior to polymerization, styrene monomers can be functionalized such that latex molecules having widely different surface properties can be readily prepared. The latex particles selected for this investigation were chosen to have similar surface charge densities so that their respective EDL interactions are comparable. Despite efforts to achieve differently sized particles having similar surface properties, it is possible that there are relative hydrophobicity differences between the particles. The relative hydrophobicity of the particles is of interest in colloid filtration experiments because the hydrophobic effect could lead to an increase in particle deposition [67-70]. Furthermore, once the particles have been conditioned with HAs it is possible to observe differences in the way each of the particles interacts with HAs and this could differentially affect the hydrophobicities of the three particles.

There are several different tests that are commonly used for the measurement of relative hydrophobicity of which the two most commonly used are contact angle and MATH tests. While contact angle measurements made on smooth and uniform surfaces have a solid theoretical basis it is still unclear what effects differential drying of the lawn [71] and the formation of surface microstructure have on measurements. Furthermore, it was decided that the quantities of nanoparticles that would be required to create "lawns" of nano-scale colloids of comparable size to those traditionally used for bacterial contact angle measurements would be financially prohibitive and wasteful.

The other of these tests, known as the MATH test, involves contacting an aqueous suspension of particles to an organic phase (hydrocarbon) and relates the relative partitioning of particles into the organic phase to those particles' relative hydrophobicities. While it was originally developed exclusively for measuring bacterial cell surface hydrophobicity [72], it has since been extended here to the testing of inorganic colloids (Microsphere Adhesion to Hydrocarbons). Since adhesion to hydrocarbon will not only be a function of hydrophobicity but also of van der Waals, electrostatic repulsion and various other short range forces, it is important that experimental conditions be chosen that minimize the impact that these other factors have on adhesion. As such it is important that MATH tests be carried out at the particles' isoelectric point to eliminate the impact that surface charge effects have on adhesion.

A.2.0 Materials and Methods

A.2.1 Materials

Sulphate Latex Microspheres: As mentioned in Section 3.1.1 Nanoparticles, sulphate latex microspheres of varying sizes (50 nm, 110 nm, and 1500 nm) and mass concentrations were purchased from Sigma-Aldrich. Solutions used were prepared in 50 mL Falcon tubes by diluting stock colloidal samples in electrolyte of varying ionic strength (1 – 100 mM KCl). The ionic strength of the electrolyte was varied through the addition of a 1 M KCl stock solution to deionized (DI) water. The number concentrations used for the 50 nm, 110 nm and 1500 nm latex colloids were respectively, 1.15×10^{11}, 1.16×10^{10} and 8.04×10^{6} particles/mL. For all experiments, pH was adjusted to the isoelectric point through addition of 12 M HCl. n-Hexadecane was selected for use as the sample hydrocarbon.

A.2.2 Methods

MATH tests were carried out in standard 10 mm glass test tubes to which were added 4 mL of n-hexadecane and 1 mL of sample latex particles suspended in electrolyte. The mixtures were agitated at maximum velocity on a Fisher-Scientific 150 W analog mini-vortex for 120 s. It is essential that test tubes be uniformly clean and to this end, they were acid washed prior to use [72]. Samples were then left to stand for 15 min to allow sufficient time for the complete partitioning of the organic phase. A Pasteur pipette was then used to carefully remove the aqueous phase and transfer it to a quartz cuvette. Absorbance of the aqueous phase was measured at 254 nm using a spectrophotometer before and after being contacted with the hydrocarbon. The process was repeated in triplicate for all experimental conditions tested. To be able to account for the absorbance of any hydrocarbons remaining in the aqueous phase and for the partitioning of HAs, control experiments were performed where electrolyte and hydrocarbon were contacted in the absence of the latex particles.

The isoelectric points for the three latex particles were determined by preparing suspensions having the same number concentration as those in the filtration experiments, with 10 mM KCl and in both the presence and absence of HAs. The pH of these

solutions was then manipulated through the addition of appropriate volumes of HCl and NaOH and a measurement of the electrophoretic mobility of the solutions was performed at each pH. Due to the loss of dispersion stability that occurs near the point of zero charge, resolution in mobility measurements is lost near this point, and as such the isolectric points for the colloids was then estimated with as much accuracy as was possible.

A.3.0 Results

As was previously discussed, MATH tests are often carried out at a particle's isoelectric point as this allows the relative hydrophobicity of the particle to be examined in the absence of electrostatic interactions. The isoelectric points of the three colloids were determined and the results of this investigation are summarized in Table 1.

Sample Name	pH	Zeta Potential (mV)	Mobility (μmcm/Vs)	Conductivity (mS/cm)
51 nm Latex	1.09	-18.20	-1.32	51.78
0.0 [mg/L]	1.47	-23.58	-1.71	16.45
10 [mM] KCl	2.47	-40.30	-2.92	3.50
	5.61	-46.63	-3.38	1.59
	11.94	-46.85	-3.39	3.63

Sample Name	pH	Zeta Potential (mV)	Mobility (μmcm/Vs)	Conductivity (mS/cm)
51 nm Latex	1.1	-6.48	-0.47	63.70
5.0 [mg/L]	1.6	-17.90	-1.30	19.40
10 [mM] KCl	2.5	-31.78	-2.30	3.55
	5.6	-48.33	-3.50	1.59
	11.7	-57.05	-4.13	2.65

Sample Name	pH	Zeta Potential (mV)	Mobility (μmcm/Vs)	Conductivity (mS/cm)
110 nm Latex	1.07	-11.02	-0.80	56.35
0.0 [mg/L]	1.56	-24.83	-1.80	18.00
10 [mM] KCl	2.45	-36.48	-2.64	3.55
	5.5	-46.23	-3.35	1.62
	11.71	-61.53	-4.46	2.83

Sample Name	pH	Zeta Potential (mV)	Mobility (μmcm/Vs)	Conductivity (mS/cm)
110 nm Latex	1.1	-8.29	-0.60	67.25
5.0 [mg/L]	1.6	-16.40	-1.19	20.23
10 [mM] KCl	2.5	-34.13	-2.47	3.58
	5.7	-55.08	-3.99	1.61
	11.8	-63.43	-4.59	3.27

Sample Name	pH	Zeta Potential (mV)	Mobility (μmcm/Vs)	Conductivity (mS/cm)
1500 nm Latex	1.09	-12.68	-0.92	52.08
0.0 [mg/L]	1.58	-40.03	-2.90	17.05
10 [mM] KCl	2.48	-73.15	-5.30	3.52
	5.6	-101.58	-7.35	1.59
	11.76	-104.50	-7.58	2.86

Sample Name	pH	Zeta Potential (mV)	Mobility (μmcm/Vs)	Conductivity (mS/cm)
1500 nm Latex	1.1	-6.31	-0.46	65.45
5.0 [mg/L]	1.5	-12.85	-0.93	21.53
10 [mM] KCl	2.5	-40.30	-2.92	3.48
	5.7	-84.00	-6.09	1.56
	12.1	-76.35	-5.53	4.13

Table 1: Isoelectic points for 50, 110 and 1500 nm latex colloids

The loss in resolution that occurs in electrophoretic mobility measurements taken near the point of zero charge may have lead to slight inaccuracies in the isoelectric points determined. Despite the possibility of inaccuracies, the ultimate goal of determining the isoelectric point was to minimize the impact that charge has on hydrophobicity

measurements and this was achieved. During the course of MATH tests, aqueous samples were intimately contacted with hydrocarbons and the partitioning of colloids between aqueous and organic phases was permitted. To determine the impact of any leftover hydrocarbon that may remain in the aqueous phase following agitation and prior to sampling and in an attempt to quantify the impact that the partitioning of HAs have on the measured absorbance, control experiments were performed involving aqueous suspensions either with or without HAs that did not contain any colloids. The results of these controls have been normalized by dividing the absorbance of samples taken following agitation with the absorbance of the samples taken beforehand. The raw data and a plot of C/C0 versus solution composition data for these control experiments have been summarized and are presented in Table 2 and Figure 8. The raw data has been included here because it is important to note the absolute value of absorbance shifts that were observed in the controls relative to the MATH tests themselves.

Controls	Absorbance: Co		Absorbance: Samples		C/Co
	Average	StDev	Average	StDev	
10 [mM]	0.0116	0.00005	0.0149	0.0006	1.2861
10 [mM] & humics	0.1459	0.0005	0.0605	0.0031	0.4145
100 [mM]	0.0121	0.0002	0.0154	0.0009	1.2730
100 [mM] & humics	0.1546	0.0018	0.0609	0.0040	0.3936

Table 2: MATH test raw data (controls)

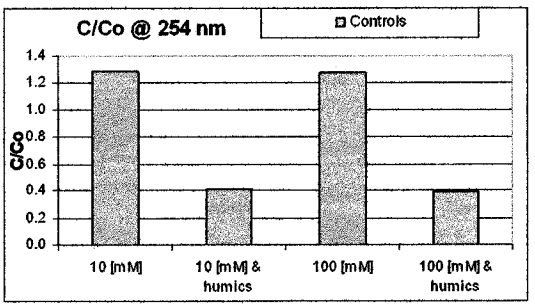

Figure 8: C/C0 versus solution composition (controls)

Inspection of these results allows certain observations to be made. When MATH tests were carried out in the absence of colloids and HAs, the presence of remnant hydrocarbon in the aqueous phase contributed to the total absorbance and resulted in C/C_0 values greater than unity. Furthermore, when MATH tests were carried out in the

absence of colloids but in the presence of HAs, a significant portion of the HAs partitioned into the organic phase resulting in C/C_0 values considerably lower than unity. While it is possible that the presence of HAs may have some effect on the separation of hydrocarbon and aqueous phases following agitation by stabilizing the dispersed organic phase, it is assumed for the sake of this investigation that the presence of HAs does not effect the amount of n-hexadecane that is remnant in the aqueous phase at the time of sampling. For the value of absorbance shift representing the partitioning of HAs to be truly representative, the absorbance shift caused by the presence of remnant hydrocarbon should first be subtracted.

MATH tests were carried out with all particle sizes at their respective isoelectric points (pH~1) and at physicochemical conditions that were representative of the range of physicochemical conditions investigated during the colloid filtration experiments in both the presence and absence of HAs. The raw data and unadjusted C/C_0 versus solution composition data for these experiments have been summarized and are presented in Table 3 and Figure 9. The raw data has been included here because it is important to note the absolute value of absorbance shifts that were observed in the controls relative to the MATH tests themselves, as was previously discussed.

Solution Composition	51 nm Latex	110 nm Latex	1500 nm Latex
	C/Co	C/Co	C/Co
10 [mM]	0.100	0.063	0.077
100 [mM]	0.072	0.084	0.208
10 [mM] & humics	0.171	0.196	0.273
100 [mM] & humics	0.186	0.186	0.295

Table 3: Unadjusted MATH test raw data (colloids)

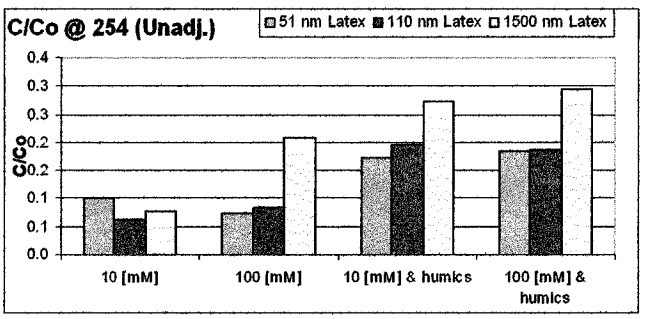

Figure 9: Unadjusted C/C0 versus solution composition (colloids)

As was previously discussed, the absorbance shift factors for the partitioning of unassociated HAs and remnant n-hexadecane determined during control experiments could then be used to adjust the data obtained with the various colloidal particles. This will ideally allow the impact of HAs and n-hexadecane partitioning that was previously mentioned to be factored out of the experimental data. This allows the impact of NOM on the relative hydrophobicity of the particles to be examined in isolation. The raw data and adjusted C/C_0 versus solution composition data for these experiments have been summarized and are presented in Table 4 and Figure 10. As before, the raw data has been included here to note the absolute value of absorbance shifts that were observed.

Solution Composition	51 nm Latex	110 nm Latex	1500 nm Latex
	Adj. C/Co	Adj. C/Co	Adj. C/Co
10 [mM]	0.088	0.052	0.068
100 [mM]	0.059	0.075	0.199
10 [mM] & humics	0.592	0.627	0.567
100 [mM] & humics	0.714	0.559	0.595

Table 4: Adjusted MATH test raw data (colloids)

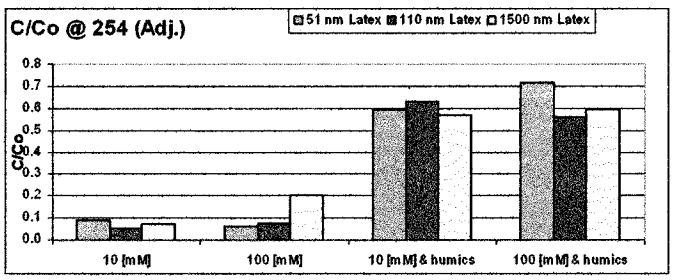

Figure 10: Adjusted C/C0 versus solution composition (colloids)

A.4.0 Conclusions and Projections to Future Works

Anomalies that were observed in the behaviour of the colloidal suspensions in the presence of HAs lead to the conclusion that some short range force (i.e., London forces, hydrophobicity, etc.) not normally considered in DLVO might be at least partly responsible. In particular, since hydrophobic interactions are suspected to be involved in

the association of HAs with the hydrophobic surfaces of the latex particles, it was decided to investigate the relative hydrophobicity of the three colloids in their presence and absence. Two of the most commonly used tests of relative hydrophobicity are contact angle and MATH tests. While contact angle measurements have a solid theoretical basis, it was decided that the quantities of nanoparticles required would be financially prohibitive and wasteful. The other of these tests, known as the MATH test, involves contacting an aqueous suspension of particles to an organic phase (hydrocarbon) and relates the relative partitioning of particles into the organic phase to those particles' relative hydrophobicities. While it was originally developed exclusively for measuring bacterial cell surface hydrophobicity [72], it has since been extended here to the testing of inorganic colloids (Microsphere Adhesion to Hydrocarbons).

Observation of the data obtained from the MATH tests confirms the expectation that the latex particles being investigated are indeed hydrophobic. Figure 10 shows that in the absence of HAs, the majority of latex particles preferentially partitioned to the organic phase, as would be expected of hydrophobic particles. In the presence of HAs, a greater fraction of the particles remained in the aqueous phase following agitation. It was concluded that the HAs acted as an organic phase dispersed within the aqueous phase and that the close association between HAs and the colloids allowed the latex particles to be sufficiently hydrophobically stabilized to remain dispersed in the aqueous phase. While this observation indicates that hydrophobicity is likely playing some kind of role in the observed behaviour of the colloids during deposition studies, the creation of a significant dispersed organic greatly complicated the interpretation of data obtained from MATH tests.

Therefore, while the results obtained from MATH tests might hint at interesting conclusions and while the extension of MATH tests to inorganic particles is likely still a viable prospect, the MATH test was found to be inappropriate for the three phase system created through the inclusion of HAs as the interpretation of data became practicably impossible.

Appendix B: Biofilms Experiments

B.1.0 Introduction

The role that microorganisms play in the mobility of pollutants and colloids in the subsurface has not been traditionally recognized despite the fact that they play a significant role in completing the cycling of the majority of the earth's nutrients. In fact, the majority of groundwater systems are home to a rich ecosystem, including invertebrate [73] and (to a lesser extent) vertebrate [74] organisms. In fact, it has been estimated that groundwater systems are home to the greatest number of rare taxa of all the earth's ecosystems [75]. Recently, an increasing amount of researchers are realizing that the most pronounced effect of microorganisms in subsurface systems lies in their tendency to form biofilms. Though biofilms are formed and inhabited by individual microbial cells, they form highly structured microenvironments including microcolonies of various species that can develop synergistic relationships [76]. Research has demonstrated that such microconsortia are capable of degrading structures far more complex than could be utilized by single members of the consortium [77]. This ability has largely been attributed to the ability of these microbes to release extracellular polymeric substances (EPS) [78]. EPS are biosynthetic polymers that mainly consists of proteins and polysaccharides, but the extracellular environment forming the biofilms can also contain substantial amounts of DNA, lipids, glycolipids and humic substances [79, 80]. Using batch-style experiments, one group found that biofilm thickness acquired a sort of quasi-steady state after approximately five days growth under high nutrient loadings. The same group also observed that the porosity of the medium decreased between 50 and 96% and permeability decreased between 92 and 98% [81]. This observation indicates that given the proper geochemistry and a sufficient supply of substrates, thick biofilms can develop and significantly alter porosity and permeability of the medium and thereby greatly affecting the transport of influent mobile colloids. However, to date there have been very few controlled laboratory investigations quantifying the effect that biofilms have on the transport and fate of colloids. And of the few such experiments that have been performed, they have yielded puzzling results as one group has observed decreased

cryptosporidium parvum oocyst removal in the presence of biofilms [82] whereas others have observed that biofilms are "sticky" and they aid in the removal of colloids [76, 83].

It was decided to design a protocol for the study of transport when the experimental system is first preconditioned with biofilms in order to facilitate future research in this arena. The initial plan was to first design an experimental protocol that could be used for homogeneously conditioning packed columns with biofilm-coating. The intent had been to then perform a selected number of filtration experiments using the nano- to micron-scale latex particles in order to be able to compare with the results obtained from earlier experiments. While it proved to be beyond the scope of this project to perform any colloid filtration experiments in biofilm preconditioned columns, the protocol is outlined below and a discussion of the works with a projection to future works is included.

B.2.0 Materials and Methods

B.2.1 Materials

Lennox Broth (LB) growth media
Potassium Chloride
Agar
Quartz sand (Sigma)
Pseudomonas aeruginosa ATCC # 27853

2x Pair of column end-pieces and fittings
2x 1.6 cm diameter glass chromatography column
Masterflex peristaltic pump
Masterflex tygon pump tubing
Syringe pump
Standard tygon tubing
Assorted Omnifit fittings and tee/4-way valves
Oven
2x Meat thermometer

2.0 L graduated cylinder

500 mL baffled Erlenmeyer flask

2x 2.0 L screw-top Erlenmeyer flask

3x 1.0 L Erlenmeyer flask

2x 250 mL Wheaton bottle

1.0 L beaker (for waste collection)

3x Magnetic stir-bar

Large weighing dishes

B.2.2 Methods

Biofilms: Pre-preparation

Pre-prepare: 1x 1.0 L Erlenmeyer flask with 20.0 g/L LB media (+ stir-bar);

2x 1.0 L screw-top Erlenmeyer flask with 2.0 g/L LB media (+ stir-bar);

1x 500 mL baffled Erlenmeyer flask with 20.0 g/L LB media;

2x 1.0 L Erlenmeyer flask with sterile deionized water;

2x 7.5g sterile and saturated sand in 250 mL Wheaton bottle;

1x 1.5% wt/v agar/20.0 g/L LB plate of *P. aeruginosa* 27853

* All transfers that expose sterile media to atmosphere (particularly inoculation) must be carried out in a Biological Safety Cabinet (BSC)

Media Preparation

- Rinse 3x 1.0 L Erlenmeyer flask with deionized water
- Rinse 1x 500 mL Baffled Erlenmeyer flask with deionized water
- Rinse 2x 1.0 L Screw-top Erlenmeyer flask + cap with deionized water

- Fill 2x 1.0 L Erlenmeyer flask with ~800 mL deionized water
- Cap flask with sponge, metal foil, autoclave tape and set aside for sterilization
    - These will be used for column flushing

- Fill 1x 1.0 L Erlenmeyer flask with a small volume of deionized water
- Rinse a large weighing dish

- Tare weighing dish on analytical balance and measure 16.0 g LB media
- Transfer media from weighing dish to flask using rinse bottle as necessary
- Shake flask manually until homogeneity of media is achieved
- Fill flask with deionized water up to 800 mL mark
- Shake flask manually
- Rinse magnetic stir-bar with deionized water and drop into media flask
- Cap flask with sponge, metal foil, autoclave tape and set aside for sterilization
    - This will be used for conditioning the column with full strength media

- Fill 1x 2.0 L graduated cylinder with a small volume of deionized water
- Rinse a large weighing dish
- Tare weighing dish on analytical balance and measure 5.0 g LB media
- Transfer media from dish to graduated cylinder using rinse bottle as necessary
- Swirl contents of graduated cylinder to manually homogenize media
- Fill graduated cylinder with deionized water up to 250 mL mark
- Swirl contents of graduated cylinder to manually homogenize media
- Transfer ~150 mL of media into 1x 500 mL baffled Erlenmeyer flask
- Cap flask with sponge, metal foil, autoclave tape and set aside for sterilization
    - This will be used to make a liquid bacterial culture from the plate

- Fill 2x 2.0 L screw-top Erlenmeyer flasks with a small volume of deionized water
- Rinse a large weighing dish
- Tare weighing dish on analytical balance and measure 3.2 g LB media
- Transfer media from weighing dish to flask using rinse bottle as necessary
- Shake flask manually until homogeneity of media is achieved
- Fill flask with deionized water up to 1600 mL mark
- Shake flask manually
- Rinse magnetic stir-bar with deionized water and drop into media flask
- Cap flask with screw-top cap and autoclave tape and set aside for sterilization
    - This will be used to maintain the growth of bacteria in the column as part of the column conditioning procedure

Sand Preparation

- Rinse 2x 250 mL Wheaton bottle + cap
- Fill 2x 250 mL Wheaton bottle with a small volume of deionized water
- Rinse a large weighing dish
- Tare dish on analytical balance and measure 2x 7.5 g prepared quartz sand
- Transfer sand from dish to flask using rinse bottle as necessary
- Fill 2x 250 mL Wheaton bottle with water up to ~ 200 mL mark
- Cap bottle with screw-top cap and autoclave tape and set aside for sterilization

Sterilization

- Sterilize media and sand using autoclave on liquid cycle
- Store 1x 1.0 L Erlenmeyer flask with 20.0 g/L LB media, 2x 1.0 L screw-top Erlenmeyer flask with 2.0 g/L LB media, 2x 1.0 L Erlenmeyer flask with deionized water and 2x 7.5g quartz sand in 250 mL Wheaton bottle at 37°C
- Set aside 1x 500 mL baffled Erlenmeyer flask with 20.0 g/L LB media for bacterial culture preparation

Bacterial Culture Preparation

- Pre-prepare 1.5% wt/v agar/20.0 g/L LB plates
- Inoculate plate from frozen culture (cryogenic tube) of *P. aeruginosa* 27853
- Label, seal and place plate in incubator at 37°C for ~24 hrs
- Remove plate from incubator and store in 4°C fridge

*It is important to ensure that the next phase of this process is carried out concurrently with column-preparation and column conditioning such that bacterial culture and sterilized column are simultaneously available

- Inoculate 1x 250 mL baffled Erlenmeyer flask with *P. aeruginosa* 27853 picked from 1.5% wt/v agar/20.0 g/L LB plate
- Return *P. aeruginosa* 27853 plate to fridge
- Place 500 mL baffled Erlenmeyer flask in incubator and shake at 200 rpm overnight for ~18hrs
- Take a sample of solution from 500 mL baffled Erlenmeyer flask and measure turbidity using UV-visible spectrophotometer at 600 nm wavelength

- Dilute sample until standardized turbidity measurement of 0.3 is achieved
- Use a 1.0 mL sample of diluted culture to inoculate 1.0 L screw-top Erlenmeyer flask with 2.0 g/L LB media as it circulates through the column (column preparation details to follow)

Biofilms: Column Preparation

- Rinse surfaces of column and lower end-pieces with 85% ethanol/15% methanol
- Wipe lower end-pieces with a kimwipe and re-rinse with 85% ethanol/15% methanol
- Fill columns until they contain a significant standing volume of ethanol
- Allow some ethanol to drain from the column to flush effluent lines of air bubbles
- Close outlet valves to prevent the emptying of the column
- Refill column with a standing volume of ethanol
- Add lower sand membrane using sterile pipette
- Fill each column with pre-saturated sand and minimal volume of water (ensure that the lower membrane is undisturbed by adding the first small quantity of sand very slowly)
- Vibrate column with back-massager to ensure homogeneous column packing
- Attach ethanol beaker inline
- Flush to waste through all valves and start flow of ethanol to end-pieces
- Rinse top end-pieces with ethanol, wipe with kimwipe and re-rinse with ethanol
- Seal column without air bubbles

Biofilms: Column Conditioning

- Flush column with ethanol for ~10PV's
- Switch to 20.0 g/L LB media beaker precondition columns with media for ~20 PV's (spin)
- Switch to 2.0 g/L media beaker and begin flushing (spin)
- Inoculate media flask with 1.0 mL of liquid culture
- Allow solution to circulate overnight ~18 hrs (spin)
- Back-flush column for ~6 hrs (spin)

- Switch to fresh 2.0 g/L media every 24 hrs and repeat steps including circulation overnight ~18 hrs and back-flush ~6 hrs
- Continue until even colour gradient is achieved across length of column

Biofilms: Column Characterization

Column Homogeneity

Once conditioned with biofilms, the goal of this protocol is to be able to perform a series of filtration experiments in order to determine the effect that biofilm conditioning has on the deposition behaviour of colloidal suspensions. However, in order to be able to compare the results of experiments carried out in separate columns, it is of paramount importance that the various columns be as homogeneously and consistently conditioned as possible. To this end, all growth parameters are controlled as tightly as possible. As is the rationale with the preparation of a growth curve, given similar inoculant volume and concentration, nutrient availability and external growth conditions (i.e. temperature, etc.) the observed growth of biofilm should be roughly equivalent between experiments. However, as a means of demonstrating that this assertion is true, it had been the intent of this project to condition a series of columns with biofilms and then characterize the distribution of bacteria throughout the column.

Ideally, after having been conditioned with biofilms, it would be possible to slowly remove the column of sand from the chromatography column and divide its length into sections. Each of these sections could then be placed into a separate Falcon tube and vortexed to liberate attached biofilms and bacteria from the surface of the sand grains. After a short settling period, it would then be possible to take a sample of the liquid solution and using plate counting techniques quantify the distribution of bacteria throughout the column. Though it may be argued by some that not all of the bacteria harvested from a biofilm community in this manner are going to be culturable, the number of bacteria that are culturable within a given slice should be comparably representative of the total number of bacteria. It had been the intention of this project to carry out this investigation and quantify bacterial distribution throughout the column but due to time constraints, this goal was not achieved.

Biofilms: Filtration Experiments

The experimental setup designed for use in these experiments incorporated a direct input for colloidal particles similar to the system that was used in the majority of my filtration experiments. This was ultimately to allow for the comparison of elution curves in the presence and absence of biofilm conditioning. However, it was decided that it would not be possible to perform filtration studies using the exact colloidal particles that were used throughout the bulk of my Masters. A UV-visible spectrophotometer has been used throughout the rest of the project to characterize the difference in turbidity between solutions influent and effluent to a column. A limitation of this equipment is that it is unable to differentiate between colloidal particles, bacterial cells and biofilm debris. This would make it impossible to compare the turbidity of influent and effluent solutions.

It was decided that a better approach would involve the use of fluorescently labelled latex particles and a fluorescent spectrophotometer. This would allow for the influent and effluent concentrations of latex particles to be characterized without overt interference from the debris present in the effluent solution. Due to time constraints and equipment acquisition delays, it was not possible to attempt these filtration studies using fluorescently labelled latex particles.

B.3.0 Conclusions and Projections to Future Work

Over the course of this project, a protocol has been developed for the conditioning of columns with biofilms in order to be able to carry out colloidal filtration studies in their presence and absence. Given a consistent column packing technique, tightly regulated growth parameters and consistent inoculants it is believed that the use of this protocol will result in comparable biofilm. However, in order to prove that this is true, quantification of the distribution of bacteria throughout the column is still required and should be the initial focus of future works. Once it has been established, use of this protocol in conjunction with fluorescently labelled latex particles and a fluorescent spectrophotometer should ultimately make an investigation into the effect of biofilm conditioning on the transport behaviour of colloidal suspensions in porous media possible.

References

1. Smit, P., Heniger, J., *Antoni van Leeuwenhoek (1632–1723) and the discovery of bacteria.* Antonie van Leeuwenhoek, 1975. **41**(1): p. 217-228.

2. Debré, P., Forster, E., *Louis Pasteur.* 1998: Johns Hopkins University Press.

3. Chiras, D.D., *Human Biology.* Medical / Nursing. 2005: Jones & Bartlett. 464.

4. Wiesner, M.R., Lowry, G.V., Alvarez, P., Dionysiou, D., Biswas, P., *Assessing the Risks of Manufactured Nanomaterials.* Environmental Science & Technology, 2006: p. 4336-4345.

5. Elimelech, M., O'Melia, C.R., *Effect of Electrolyte Type on the Electrophoretic Mobility of Polystyrene Latex Colloids.* Colloids and Surfaces, 1990. **44**: p. 165-178.

6. Penners, N.H.G., Koopal, L.K., *The effect of particle size on the stability of haematite ([alpha]-Fe2O3) hydrosols.* Colloids and Surfaces, 1987. **28**: p. 67.

7. Reerink, H., Overbeek, J.Th.G., *The rate of coagulation as a measure of the stability of silver iodide sols.* Discuss. Faraday Soc., 1954. **18**: p. 74 - 84.

8. Wiese, G.R., Healy, T.W., *Effect of Particle Size on Colloid Stability.* Trans Faraday Soc, 1970. **66**: p. 490-499.

9. Elimelech, M., O'Melia, C.R., *Effect of Particle Size on Collision Efficiency in the Deposition of Brownian Particles with Electrostatic Energy Barriers.* Langmuir, 1990. **6**: p. 1153-1163.

10. Elimelech, M., *Effect of Particle Size on the Kinetics of Particle Deposition under Attractive Double Layer Interactions.* Journal of Colloid Interface Science, 1994. **164**: p. 190-199.

11. Lecoanet, H.F., Bottero, J.-Y., Wiesner, M., *Laboratory Assessment of the Mobility of Nanomaterials in Porous Media.* Environmental Science and Technology, 2004. **38**(19): p. 5164-5169.

12. Tufenkji, N., Elimelech, M., *Correlation Equation for Predicting Single-Collector Efficiency in Physicochemical Filtration in Saturated Porous Media.* Environmental Science and Technology, 2004. **38**(2): p. 529-536.

13. Yao, K.M., Habibian, M.T., O'Melia, C.R., *Water and Waste Water Filtration: Concepts and Applications.* Environmental Science and Technology, 1971. **5**(11): p. 1105-1112.

14. Prieve, D.C., Ruckenstein, E., *Effect of London Forces upon the rate of Deposition of Brownian Particles.* AIChE Journal, 1974. **20**: p. 1178-1187.

15. Rajagopalan, R., Tien, C., *Trajectory analysis of deep-bed filtration with the sphere-in-cell porous media model.* AIChE Journal, 1976. **22**(3): p. 523-533.

16. Derjaguin, B.V., Landau, L.D., *USSR Acta Physicochim.* 1941. **14**: p. 633.

17. Verwey, E.J.W., Overbeek, J.Th.G., *Theory of the Stability of Lyophobic Colloids.* 1948.

18. Hancock, P.J., *Aquifers and hyporheic zones: Towards an ecological understanding of groundwater.* Hydrogeology journal, 2005. **13**(1): p. 98.

19. McCarthy, J.F., McKay, L.D., *Colloid Transport in the Subsurface: Past, Present, and Future Challenges.* Vadose Zone J, 2004. **3**(2): p. 326-337.

20. Ranville, J.F., *Particle-size and element distributions of soil colloids: Implications for colloid transport.* Soil Science Society of America journal, 2005. **69**(4): p. 1173.

21. Ryan, J.N., Elimelech, M., *Colloid mobilization and transport in groundwater.* 1996. **107**: p. 1-56.

22. Chen, Z., Cai, Y., Solo-Gabriele, H., Snyder, G.H., Cisar, J.L., *Interactions of Arsenic and the Dissolved Substances Derived from Turf Soils.* Environ. Sci. Technol., 2006. **40**(15): p. 4659-4665.

23. Mylon, S.E., Chen, K.L., Elimelech, M., *Influence of Natural Organic Matter and Ionic Composition on the Kinetics and Structure of Hematite Colloid Aggregation: Implications to Iron Depletion in Estuaries.* Langmuir, 2004. **20**(21): p. 9000-9006.

24. Lippold, H., Mansel, A., Kupsch, H., *Influence of trivalent electrolytes on the humic colloid-borne transport of contaminant metals: competition and flocculation effects.* Journal of Contaminant Hydrology, 2005. **76**(3-4): p. 337.

25. Mibus, J., Sachs, S., Pfingsten, W., Nebelung, C., Bernhard, G., *Migration of uranium(IV)/(VI) in the presence of humic acids in quartz sand: A laboratory column study.* Journal of Contaminant Hydrology, 2007. **89**(3-4): p. 199.

26. Totsche, K.U., Kogel-Knabner, I., *Mobile Organic Sorbent Affected Contaminant Transport in Soil: Numerical Case Studies for Enhanced and Reduced Mobility.* Vadose Zone J, 2004. **3**(2): p. 352-367.

27. Wilkinson, K.J., Negre, J.-C., Buffie, J., *Coagulation of colloidal material in surface waters: the role of natural organic matter.* Journal of Contaminant Hydrology, 1997. **26**: p. 229-243.

28. Myneni, S.C.B., Brown, J.T., Martinez, G.A., Meyer-Ilse, W., *Changes in the Macromolecular Structures of Isolated Humic Substances Under Different Solution Chemical Conditions.* American Chemical Society, 1999. **217**.

29. Ghosh, K., Schnitzer, M., *Macromolecular Structures of Humic Substances.* Soil Science, 1980. **129**(5): p. 266-276.

30. Einstein, A., *Über die von der molekularkinetischen Theorie der Wärme geforderte Bewegung von in ruhenden Flüssigkeiten suspendierten Teilchen.* Ann. Phys., 1905. **17**(549).

31. Bohren, C.F., Huffman, D., *Absorption and scattering of light by small particles.* 1983, New York: John Wiley.

32. Morfesis, A., Rodolewicz, J., Fraser, M., *Particle Sizing by Dynamic Light Scattering*, in *Zetasizer Nano Z/ZS Training Course*. 2006, Malvern Instruments USA. p. 83.

33. Morfesis, A., Watson, L., Fraser, M., *The Zeta Potential*, in *Zetasizer Nano Z/ZS Training Course*. 2006, Malvern Instruments USA. p. 83.

34. Taylor, J.R., Zafiratos, C.D., Dubson, M.A., *Modern Physics for Scientists and Engineers*. 2004, Upper Saddle River: Prentice Hall.

35. Minor, M., van der Linde, A.J., van Leeuwen, H.P., Lyklema, J., *Dynamic Aspects of Electrophoresis and Electroosmosis: A New Fast Method for Measuring Particle Mobilities.* Journal of Colloid and Interface Science, 1997. **189**(2): p. 370.

36. Litton, G.M., Olson, T.M., *Colloid Deposition Rates on Silica Bed Media and Artifacts Related to Collector Surface Preparation Methods.* Environmental Science and Technology, 1993. **27**(1): p. 185-193.

37. Rand, G.M., Wells, P.G., McCarty, L.S., *Fundamentals of Aquatic Toxicology: Effects, Environmental Fate, and Risk Assessment*, ed. G.M. Rand. 1995: Taylor & Francis. 1125.

38. Assemi, S., *Investigation of adsorbed humic substances using atomic force microscopy.* Colloids and surfaces. A, Physicochemical and engineering aspects, 2004. **248**(1-3): p. 17.

39. Tufenkji, N., Elimelech, M., *Deviation from the Classical Colloid Filtration Theory in the Presence of Repulsive DLVO Interactions.* Langmuir, 2004. **20**: p. 10818-10828.

40. Gregory, J., *Approximate expressions for retarded van der waals interaction.* Journal of Colloid and Interface Science, 1981. **83**(1): p. 138.

41. Hogg, R., Healy, T.W., Fuerstenau, D.W., *Mutual Coagulation of Colloidal Dispersions.* Trans Faraday Soc, 1966. **62**(522P): p. 1638-1651.

42. Gregory, J., *Interaction of unequal double layers at constant charge.* Journal of Colloid and Interface Science, 1975. **51**(1): p. 44.

43. Tiller, C.L.a.O.M., C.R., *Natural organic matter and colloidal stability: Models and measurements.* Colloids and Surfaces: A, 1993. **73**: p. 89-102.

44. Tipping, E.a.H., D.C., *The effect of adsorbed humic substances on the colloid stability of haematite particles.* Colloid. Surface, 1982. **5**: p. 85-92.

45. Van Den Hoven, T.J.J., Bijsterbosch, B.H., *Streaming currents, streaming potentials and conductances of concentrated dispersions of negatively-charged, monodisperse polystyrene particles. Effect.* Colloids and Surfaces, 1987. **22**(2): p. 171.

46. Van Der Put, A.G., Bijsterbosch, B.H., *Electrokinetic measurements on concentrated polystyrene dispersions and their theoretical interpretation.* Journal of Colloid and Interface Science, 1983. **92**(2): p. 499.

47. Zukoski, C.F., Saville, D.A., *The interpretation of electrokinetic measurements using a dynamic model of the stern layer: I. The dynamic model.* Journal of Colloid and Interface Science, 1986. **114**(1): p. 32.

48. Zukoski, C.F., Saville, D.A., *The interpretation of electrokinetic measurements using a dynamic model of the stern layer: II. Comparisons between theory and experiment.* Journal of Colloid and Interface Science, 1986. **114**(1): p. 45.

49. Elimelech, M., *Ph.D. Dissertation.* Johns Hopkins University, 1989.

50. Honig, E.P., Roebersen, G.J., Wiersema, P.H., *Effect of hydrodynamic interaction on the coagulation rate of hydrophobic colloids.* Journal of Colloid and Interface Science, 1971. **36**(1): p. 97.

51. Barchini, R., van Leeuwen, H.P., Lyklema, J., *Electrodynamics of Liposome Dispersions.* Langmuir, 2000. **16**(22): p. 8238-8247.

52. Dukhin, S.S., Lyklema, J., *Dynamics of colloid particle interaction.* Langmuir, 1987. **3**(1): p. 94-98.

53. Lyklema, J., van Leeuwen, H.P., Minor, M., *DLVO-theory, a dynamic re-interpretation.* Advances in Colloid and Interface Science, 1999. **83**(1-3): p. 33.

54. Prieve, D.C., Lin, M.M.J., *The effect of a distribution in surface properties on colloid stability.* Journal of Colloid and Interface Science, 1982. **86**(1): p. 17.

55. Prieve, D.C., Ruckenstein, E., *Role of surface chemistry in primary and secondary coagulation and heterocoagulation.* Journal of Colloid and Interface Science, 1980. **73**(2): p. 539.

56. Tobiason, J.E., *Chemical effects on the deposition of non-Brownian particles.* Colloids and Surfaces, 1989. **39**(1): p. 53.

57. Hogg, R., Yang, K.C., *Secondary coagulation.* Journal of Colloid and Interface Science, 1976. **56**(3): p. 573.

58. Payatakes, A.C., Tien, C., Turian, R.M., *Trajectory calculation of particle deposition in deep bed filtration: Part I. Model formulation.* AIChE Journal, 1974. **20**(5): p. 889-900.

59. Payatakes, A.C., Tien, C., Turian, R.M., *Trajectory calculation of particle deposition in deep bed filtration: Part II. Case study of the effect of the dimensionless groups and comparison with experimental data.* AIChE Journal, 1974. **20**(5): p. 900-905.

60. Spielman, L.A., Cukor, P.M., *Deposition of non-Brownian particles under colloidal forces.* Journal of Colloid and Interface Science, 1973. **43**(1): p. 51.

61. Shulepov, S.Y., Frens, G., *Surface Roughness and the Particle Size Effect on the Rate of Slow, Perikinetic Coagulation.* Journal of Colloid and Interface Science, 1995. **170**(1): p. 44.

62. Shulepov, S.Y., Frens, G., *Surface Roughness and Particle Size Effect on the Rate of Perikinetic Coagulation: Experimental.* Journal of Colloid and Interface Science, 1996. **182**(2): p. 388.

63. Katainen, J., Paajanen, M., Ahtola, E., Pore, V., Lahtinen, J., *Adhesion as an interplay between particle size and surface roughness.* Journal of Colloid and Interface Science, 2006. **304**(2): p. 524.

64. Rabinovich, Y.I., Adler, J.J., Ata, A.Singh, R.K., Moudgil, B.M., *Adhesion between Nanoscale Rough Surfaces: I. Role of Asperity Geometry.* Journal of Colloid and Interface Science, 2000. **232**(1): p. 10.

65. Rabinovich, Y.I., Adler, J.J., Ata, A.Singh, R.K., Moudgil, B.M., *Adhesion between Nanoscale Rough Surfaces: II. Measurement and Comparison with Theory.* Journal of Colloid and Interface Science, 2000. **232**(1): p. 17.

66. Redman, J.A., Walker, S. L., and Elimelech, M., *Bacterial Adhesion and Transport in Porous Media: Role of the Secondary Energy Minimum.* Environ. Sci. Technol., 2004. **38**(6): p. 1777-1785.

67. Breiner, J.M., Anderson, M.A., Tom, H.W.K., Graham, R.C., *Properties of Surface-Modified Colloidal Particles.* Clays and Clay Minerals, 2006. **54**(1): p. 12-24.

68. Han, J., Jin, Y., Willson, C.S., *Virus Retention and Transport in Chemically Heterogeneous Porous Media under Saturated and Unsaturated Flow Conditions.* Environ. Sci. Technol., 2006. **40**(5): p. 1547-1555.

69. McNamee, C.E., Pyo, N., Higashitani, K., *Atomic Force Microscopy Study of the Specific Adhesion between a Colloid Particle and a Living Melanoma Cell: Effect of the Charge and the Hydrophobicity of the Particle Surface.* Biophys. J., 2006. **91**(5): p. 1960-1969.

70. Simovic, S., Prestidge, C.A., *Nanoparticles of Varying Hydrophobicity at the Emulsion Droplet-Water Interface: Adsorption and Coalescence Stability.* Langmuir, 2004. **20**(19): p. 8357-8365.

71. Rosenberg, M., *Microbial adhesion to hydrocarbons: twenty-five years of doing MATH.* FEMS Microbiology Letters, 2006. **262**(2): p. 129-134.

72. Rosenberg, M., Gutnick, D., Rosenberg, E., *Adherence of bacteria to hydrocarbons: A simple method for measuring cell-surface hydrophobicity.* FEMS Microbiology Letters, 1980. **9**(1): p. 29.

73. Botosaneau, L., *A faunistic, distributional and ecological synthesis of the world fauna inhabiting subterranean waters.* Stygofauna Mundi, 1986.

74. Romero, A., *Scientists prefer them blind: the history of hypogean fish research.* Environmental Biology Fish, 2001. **62**: p. 43-71.

75. Gilbert, J., Deharveng, L., *Subterranean ecosystems: A truncated functional biodiversity.* BioScience, 2002. **52**: p. 473-481.

76. Strathmann, M., Leon-Morales, C.F., Flemming, H.-C., *Influence of biofilms on colloid mobility in the subsurface*, in *Colloidal Transport in Porous Media*, F.H. Frimmel, von der Kammer, F., Flemming, H.-C., Editor. 2007, Springer-Verlag: Berlin (Germany).

77. Wolfaardt, G.M., Lawrence, J.R., Robarts, R.D., Caldwell, D.E., *The role of interactions, sessile growth, and nutrient amendments on the degradative efficiency of a microbial consortium.* Can J Microbiol, 1994. **40**: p. 331-340.

78. Geesey, G.C., *Microbial exopolymers: ecological and economic considerations.* ASM News, 1982. **48**: p. 9-14.

79. Jahn, A., Nielsen, P.H., *Extraction of extracellular polymeric substances (EPS) from biofilms using a cation exchange resin.* Wat Sci Technol, 1995. **32**(8): p. 157-164.

80. Nielsen, P.H., Jahn, A., Palmgren, R., *Conceptual model for production and composition of exopolymers in biofilms.* Wat Sci Technol, 1997. **36**(1): p. 11-19.

81. Cunningham, A.B., Characklis, W.G., Abedeen, F., Crawford, D., *Influence of biofilm accumulation on porous media hydrodynamics.* Environ Sci Technol, 1991. **25**: p. 1305-1311.

82. Hozalski, R.M., Dai, X., *Investigation of factors affecting the removal of Cryptosporidium parvum oocysts in porous media filters.* WRC Technical, 2001. **142**: p. 17-24.

83. Sutherland, I.W., *Biofilm exopolysaccharides: a strong and sticky framework.* Microbiology, 2001. **147**(1): p. 3-9.